^{17}O and ^{13}C NMR Spectra of Stable Simple Enols[1]

Joseph Frey,[a] Irina Eventova,[a] Zvi Rappoport*,[a] Thomas Müller,[b] Yoshio Takai[c] and Masami Sawada*,[c]
[a] *Department of Organic Chemistry, The Hebrew University, Jerusalem 91904, Israel*
[b] *Department of Chemistry, Technion-Israel Institute of Technology, Haifa 32000, Israel*
[c] *Material Analysis Center, The Institute of Scientific and Industrial Research, Osaka University, Mihogaoka, Ibaraki, Osaka 567, Japan*

---

^{17}O NMR spectra of twelve stable simple enols **1** [Ar_2C=C(R)OH, Ar = crowded aryl group, R = H (**1c**, Ar = Mes), Bu^t, *m*- and *p*-substituted aryl, mesityl] were measured in $CDCl_3$ and of six of them in [$^2H_6$] DMSO. ^{13}C spectra of all the enols were measured in both solvents. These are the first values measured for enols not strongly intramolecularly hydrogen bonded. The $\delta(^{17}O)$ values in $CDCl_3$ are divided into three groups which parallel the steric bulk of R: (*i*) 70.5–74.9 when R = H; (*ii*) 84.1–87.4 when R = *m*- and *p*-substituted aryl; (*iii*) 93.0–98.5 ppm for R = Bu^t, mesityl (Mes). $\Delta\delta O = \delta(^{17}O)$ [[$^2H_6$]DMSO] − $\delta(^{17}O)$ [$CDCl_3$] = 7–10 for group (*i*), *ca.* 3 for group (*ii*) and −17 for trimesitylethenol **1l**. IGLO calculations on CH_2=CHOH (**4**) give a shallow parabola for the $\delta(^{17}O)$ *vs.* the C=C–O–H torsional angle θ plot, with maxima at $\theta = 0$ and 180° (*syn* and *anti* planar conformations) and a minimum at $\theta = 90°$. $\delta(^{13}C\text{-}2)$ values show an approximate mirror-image change while $\delta(^{13}C\text{-}1)$ changes slightly with θ. Calculation on the solvates **4**·O=SH_2 with *syn*, *anti* and perpendicular conformations show trends similar to those for uncomplexed **4** with upfield shifts of $\delta(^{17}O, ^{13}C\text{-}2)$ and downfield shift of $\delta(^{13}C\text{-}1, ^1H)$ in all conformations. When the calculations also included the effect of the reaction field, the $\delta(^{17}O)$ values of the perpendicular and *anti* conformations differ little from those of uncomplexed **4**. PM3 calculations for four enols including **1c** and **1l** also show a minimum at $\theta = 90°$ and the plot of Δ_fH for **1c** and **1l** *vs.* θ resemble the calculated energy (by MP2/6-311G**) *vs.* θ plot for **4**. No correlation exists between the Ar–C=C torsion angles or λ_{max} of the enols with $\delta(^{17}O)$, but the polar effect of the α-substituent affects the $\delta(^{17}O)$ values. The solvent effect is ascribed to OH–[$^2H_6$]DMSO hydrogen bonding, accompanied by a conformational change from *syn*-periplanar in $CDCl_3$ to mainly *anti*-clinal in [$^2H_6$]DMSO. A lower association with DMSO for bulkier Rs and an accompanying change of θ towards 90° qualitatively account for the $\Delta\delta O$ values. Several correlations between the $\delta(^{17}O)$, $\delta(^1H)$ and $\delta(^{13}C)$ shifts or of $\delta(^{13}C)$ and Hammett's σ values were found.

Steric effects play a dominant role in the chemistry of stable bulky aryl-substituted simple enols **1**.[2] This enables isolation of

$$Ar^1Ar^2C{=}C(OH)R$$

1

the enols by increasing their thermodynamic and kinetic stabilities relative to the corresponding carbonyl compounds.[2] When R = H, alkyl, there are linear relationships between the $\Delta G°$ for keto $\rightleftharpoons$ enol equilibria,[3a] the cosines of the Ar–C=C torsional angles,[3b] the R–C=C bond angles,[3b] or the rotational barriers around the Ar–C= bonds[3b] and Taft's steric parameter *Es*. Association constants of the enols with a dimethyl sulfoxide (DMSO) solvent decrease monotonously with the increased bulk of R.[4] Hence, it is interesting to search for the influence of steric effects on other properties of the enols.

Promising probes for steric effects are substituent chemical shifts (SCS) in NMR spectroscopy. The $\delta(^1H)$ of the hydroxy proton of **1** in [$^2H_6$] DMSO correlates with the bulk of an aliphatic group R, although aromatic R's have additional influence, probably *via* their ring-current effect.[5] Several ^{13}C NMR spectra were recorded for enols **1** in $CDCl_3$ but not systematically.[6] Many $\delta(^{13}C)$ values are available for non-simple enols.[6]

Another possible probe are the ^{17}O chemical shifts of the enolic oxygen.[7] ^{17}O Shifts served as probes for steric effects, both when torsion angles, *e.g.* of aryl groups conjugated to a carbonyl group, are changed[8a,b] and in rigid systems such as 2-substituted pyridine *N*-oxides.[8c]

The situation with enols **1** is more complex. The O–C=C moiety is planar and changes in the β-Ar–C=C torsional angles are at a more remote site than in carbonyl systems. With α-substituents R, the proximity of R to the geminal oxygen in the crowded enols **1**, is reminiscent of the situation in rigid systems. Consequently, a correlation between the steric environment around the OH and $\delta(^{17}O)$ may exist.

^{17}O data for simple enols are not available and even data on related non-hydrogen bonded phenols are recent.[9] In contrast, ^{17}O shifts of several enols stabilized by intramolecular hydrogen bonding to a carbonyl group were measured even in the early days of ^{17}O NMR spectroscopy. For example, for the enolic OH of acetylacetone $\delta(^{17}O) = 269$.[10] The high δ value is due to a fast keto $\rightleftharpoons$ enol equilibria with the C=O group whose $\delta(^{17}O)$ is high and similar equilibria in many dicarbonyl compounds prevented observation of a discrete enol ^{17}O signal.[11] However, for RC(OH)=$CHCO_2Et$ the $\delta(^{17}O)$ values of the enolic oxygen are 124.0 (R = Me), 109.0 (R = Ph) and 96.0 (R = CF_3).[12] The deshielding compared with aliphatic alcohols [MeOH $\delta(^{17}O) = -37$][13] was ascribed to intramolecular hydrogen bonding to the C=O.

Consequently, we studied the ^{17}O and ^{13}C spectra of enols **1a**–**l** which differ in the nature of both the α- and the β-substituents and in the steric environment around the hydroxy group and where *strong intramolecular* hydrogen bonding is absent.[4,5]

Results

The ^{17}O chemical shifts of **1a**–**l** having varying electronic and steric effects were measured in $CDCl_3$ where an intramolecular

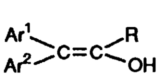

1a: $Ar^1 = Ar^2$ = Tip; R = H
1b: $Ar^1 = Ar^2 = Br_2Mes$; R = H
1c: $Ar^1 = Ar^2$ = Mes; R = H
1d: $Ar^1 = Ar^2 = C_6Me_5$; R = H
1e: $Ar^1 = Ar^2$ = Mes; R = *m*-ClC_6H_4
1f: $Ar^1 = Ar^2$ = Mes; R = Ph
1g: $Ar^1 = Ar^2$ = Mes; R = *p*-$MeOC_6H_4$
1h: $Ar^1 = Ar^2$ = Mes; R = *p*-$CF_3C_6H_4$
1i: $Ar^1 = Ar^2$ = Mes; R = Bu^t
1j: $Ar^1 = Ar^2 = C_6Me_5$; R = Bu^t
1k: Ar^1 = Ph; Ar^2 = R = Mes
1l: $Ar^1 = Ar^2$ = R = Mes

Mes = Mesityl (2,4,6-$Me_3C_6H_2$)
Tip = Tipyl (2,4,6-$Pr^i_3C_6H_2$)

bond exists between the OH and the *cis* Ar group.[4,5] Six $\delta(^{17}O)$ values were also measured in [$^2H_6$] DMSO where there is evidence for enol–DMSO intermolecular hydrogen bonding.[4,5] In view of a possible correlation with ^{13}C substituent chemical shifts (SCS) and with UV data the $\delta(^{13}C)$ of the enols and highest λ_{max} for four representative enols were also measured. The $\delta(^{17}O)$, $\delta(^{13}C\text{-}1)$ and $\delta(^{13}C\text{-}2)$ values, $\delta(^1H)$ values from previous work and λ_{max} values are given in Table 1.

$\delta(^{17}O)$ *Values in* $CDCl_3$.—No OH coupling was observed. Depending on the $\delta(^{17}O)$ value in $CDCl_3$, the enols can be divided into three groups: (*i*) four α-H-enols where $\delta(^{17}O)$ = 72.7 ± 2.2. (*ii*) Four α-*m*-X and α-*p*-X aryl-substituted enols where $\delta(^{17}O)$ = 85.7 ± 1.7. (*iii*) Two α-mesityl and two α-*tert*-butyl-substituted enols where $\delta(^{17}O)$ = 93.0–98.5. The $\delta(^{17}O)$ values span a range of 28 ppm between the extremes. The signals which were measured at 50 °C are broad and the estimated error in $\delta(^{17}O)$ values is ± 1 ppm. Hence, discussion of small SCS differences within each group is unwarranted. Specific comments are as follows:

Group (*i*) with the higher field $\delta(^{17}O)$ values represent all the least hindered α-H ethenols. Compared with the β,β-dimesityl derivative (**1c**) it includes the β-dibromomesityl electron-withdrawing groups in **1b**, or the modestly electron donating β-pentamethylphenyl groups in **1d**. X-ray data show that the effect of buttressing on the geometry of **1b** and **1d** is not large and similar for both derivatives.[14] The resulting ^{17}O shifts are upfield in **1b** and downfield in **1d**, but the effects are small. The lowest $\delta(^{17}O)$ value is for the ditipyl derivative **1a** where the *o*-Pr^i-groups are both bulkier and more electron donating than the *o*-Me groups in **1b–d**. Since the gross geometries of **1a** and **1d** do not differ much[15] the 4.4 ppm difference between the $\delta(^{17}O)$ values of these enols probably reflects the operation of both electron donation and steric effect near the oxygen.

The $\delta(^{17}O)$ value for phenol, the aromatic analog of enols, is at 73.5 in the range of group (*i*). This is not surprising since PhOH sterically resembles the enols of group (*i*) more than the other enols. Unfortunately, $\delta(^{17}O)$ values for *m*-Br, *m*-Me, *m*,*m*'-Br_2 substituted phenols, for comparison with the SCS on the enolic OH, are unavailable.

Group (*ii*) contains the four 2,2-dimesityl-1-C_6H_4X ethenols **1e–h**. The $\delta(^{17}O)$ values do not follow a Hammett-type relationship since their order for X is *p*-CF_3 > *p*-OMe > H > *m*-Cl. This may be due to the combined errors of ± 2 ppm in the values which cover only 3.3 ppm.

Group (*iii*) with the highest $\delta(^{17}O)$ values includes enols with the bulky α-Bu^t and α-Mes substituents. The $\delta(^{17}O)$ value for the α-*tert*-butyl derivative (**1i**) is 19.5 ppm higher than for the α-H derivative (**1c**). Comparison of α-Mes (**1l**) with α-H (**1c**) and α-Ph (**1f**) derivatives shows 25 and 14 ppm difference, respectively. The smaller β-Ph (in **1k**) decreases $\delta(^{17}O)$ by 2 ppm compared with β-Mes (in **1l**). Formally, a steric bulk at C-2 results in increased $\delta(^{17}O)$ values.

The concentration-dependence of $\delta(^{17}O)$ values was investigated since a dilution effect on $\delta(^{17}O)$ value of PhOH in $CDCl_3$ was noted.[16] We found the $\delta(^{17}O)$ value of PhOH in 10% (*w*/*v*) in $CDCl_3$ at 50 °C at 73.5 ppm and in the neat *vs.* external $H_2{}^{17}O$ reference at 76.0 ppm. The values for **1l** in [$^2H_6$]DMSO at 0.25 and 0.5 mol dm^{-3} were identical. Consequently, minor concentration differences between the measured $\delta(^{17}O)$ values for different enols could be neglected.

$\delta(^{17}O)$ *Values in* [$^2H_6$]*DMSO*.—Hydrogen bond accepting solvents change both the C=C–OH conformation[4] and the electron density at the oxygen. Consequently, $\delta(^{17}O)$ values were also measured for the representatives of each group, *i.e.*, **1c–f**, **1i** and **1l**, and for PhOH in [$^2H_6$]DMSO at 80 °C. Due to broadening a signal for **1j** could not be detected and the error in $\delta(^{17}O)$ value for **1i** was unusually large (± 5 ppm). The data and the solvent induced shifts $\Delta\delta O = \delta([^2H_6]DMSO) - \delta(CDCl_3)$ values are given in Table 1. The $\delta(^{17}O)$ values in [$^2H_6$]DMSO cover a narrower range (81–94 ppm) than in $CDCl_3$. The $\Delta\delta O$ values differ for the three groups, being 10 for PhOH, 7 and 10 for group (*i*), *ca.* 3 for group (*ii*) and 1 (± 5 ppm) for **1i** and − 17 for **1l** of group (*iii*).

$\delta(^{17}O)$ *Values for Polymesitylvinyl Methyl Ethers*.—In order to understand the large difference of the $\Delta\delta O$ values of **1c** and **1l** the methyl ethers **2a–c** were prepared. Unfortunately, the ^{17}O signals in [$^2H_6$]DMSO could not be detected due to broadening. The $\delta(^{17}O)$ values in $CDCl_3$ of 49 ppm for **2a** and 56 ppm for both **2b** and **c** were detected only at high concentrations and were very broad.

Mes(Ar)C=C(OMe)R

2a: Ar = Mes, R = H

2b: Ar = R = Mes

2c: Ar = Ph, R = Mes (*Z* isomer)

$\delta(^{17}O)$ *Values of* 2,4,6-*Trialkyl Benzyl Alcohols*.—For evaluating the effect of *o*-alkyl substituents on the $\delta(^{17}O)$ shift of simpler systems, the shifts of benzyl alcohol **3a**, and its 2,4,6-trialkyl substituted derivatives **3b–d** were measured. The values obtained at 100 mg per cm^3 concentration in $CDCl_3$ at 50 °C against an external $H_2{}^{17}O$ reference are given.

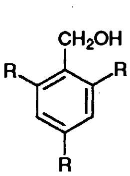

	$\delta(^{17}O)$
3a R = H	9 ± 1
b R = Me	10 ± 1
c R = Pr^i	19 ± 1
d R = Bu^t	32 ± 1

Whereas substitution of **3a** by three Me groups results in a negligible shift, substitution by bulkier alkyl groups causes an appreciable downfield shift, which increases with the bulk of the alkyl group. A significant part of the 22 ppm shift between R = Me and R = Bu^t seems of steric origin.

Unfortunately, the $\delta(^{17}O)$ signals of **3a–d** in [$^2H_6$]DMSO are too close to the dominant [$^2H_6$]DMSO signal at *ca.* 20 ppm. Consequently, no signal was observed for **3d** in [$^2H_6$]-DMSO at 80 °C.

Table 1 ^{17}O, ^{13}C and ^{1}H chemical shifts for stable enols **1** in $CDCl_3$ or in [$^2H_6$]DMSO[a,b]

	$\delta(^{17}O)$			$\delta(^{13}C\text{-}1)$	$\delta(^{13}C\text{-}2)$	$\delta(^{13}C\text{-}1)$	$\delta(^{13}C\text{-}2)$			$\delta(^{1}HO)$		λ_{max}/nm	
No.	$CDCl_3$[c]	DMSO[d]	$\Delta\delta O$[e]	in $CDCl_3$		in [$^2H_6$]DMSO		$\Delta\delta C$-1[e]	$\Delta\delta C$-2[e]	$CDCl_3$	[$^2H_6$]DMSO	hexane(log ε)	$CHCl_3$
1a	70.5			144.02	110.93	144.70	108.62	0.68	−2.31	4.72	8.92		
1b	71.9			147.19	114.99	149.96	113.08	2.77	−1.91	4.78	9.97	259 (4.18)[f]	
1c	73.5	81	7	144.10	113.24	144.92	110.82	0.82	−2.42	4.66	9.17	252 (4.23)[g]	254
1d	74.9	85	10	145.15	115.60	145.76	113.57	0.61	−2.03	4.73	8.83		
1e	84.1	87	3	148.87	112.72	149.96	113.08	1.09	+0.36	5.18	8.67		
1f	84.6	88[h]	3	150.32	111.52	151.54	111.67	1.22	+0.15	5.17	8.51	310 (4.21)	*ca.* 313
1g	86.6			150.16	110.29	151.35	110.36	1.19	+0.07	5.12	8.38		
1h	87.4			148.90	113.47	150.08	113.81	1.18	+0.34	5.21	8.78		
1i	93.0	94[i]	1[i]	156.68	108.08	156.73	108.28	0.05	+0.20	4.88	7.30	257 (4.04)[k]	259
1j	94.1	*j*		156.05	111.18	155.95	111.01	−0.10	−0.17	4.91	6.91		
1k	96.6			147.29	114.70	147.82	113.20	0.53	−1.50	4.72	8.28		
1l	98.5	81[l]	−17	148.66	114.45	149.26	113.86	0.60	−0.59	5.20	8.34	288 (3.58)	*ca.* 280

[a] References for $\delta(^{17}O)$: external $H_2{}^{17}O$ in both $CDCl_3$ and [$^2H_6$]DMSO; errors ± 1 ppm; reference for $\delta(^{13}C)$: TMS. [b] $\delta(^{17}O)$ PhOH in $CDCl_3$ = 73.5 and in [$^2H_6$]DMSO = 83.6 ppm (sharp signal, half width 500 Hz). [c] At 50 °C. [d] At 80 °C; samples are 100–200 mg cm^{-3}; for **1c**, **1d** and **1l** the half-widths of the signals are *ca.* 500 Hz, but for **1e**, **1f** and **1i** they are relatively broad (half width *ca.* 1500 Hz). [e] $\Delta\delta O = \delta(^{17}O)$ ([$^2H_6$]DMSO) − $\delta(^{17}O)$ ($CDCl_3$); $\Delta\delta C = \delta(^{13}C)$ ([$^2H_6$]DMSO) − $\delta(^{13}C)$ ($CDCl_3$). [f] Ref. 14. [g] Ref. 3(*a*); an absorption at 274 ± 4 nm (log ε > 3.2) superimposed on the main absorption may represent a longer wavelength maximum. [h] Signal could not be observed at a concentration of 160 mg cm^{-3} solvent, but a broad peak was observed for 200 mg cm^{-3} [$^2H_6$]DMSO. [i] Very broad signal with low reproducibility was observed. The error in $\delta(^{17}O)$ is ± 5 ppm. [j] No signal was detected in [$^2H_6$]DMSO at a saturated solution of 100 mg cm^{-3}. [k] Ref. 3(*a*); a shoulder at λ_{max} *ca.* 290 nm may represent a longer wavelength maximum. [l] Average of 3 independent measurements: 81.5 and 80.7 ppm at 100 mg cm^{-3} [$^2H_6$]DMSO and 81.0 ppm at 200 mg cm^{-3} [$^2H_6$]DMSO.

Temperature Effect on $\delta(^{17}O)$ *Values of* 1,4-*Dioxane*.—Since the $\delta(^{17}O)$ values were measured at 50 °C in $CDCl_3$ and at 80 °C in $[^2H_6]$DMSO, the $\Delta\delta O$ values may arise from a temperature effect. Unfortunately, due to viscosity broadening of the signals, measurements in $[^2H_6]$DMSO at 50 °C are impractical and several spectra could not be obtained even at 80 °C.

A related problem is that the signal for the external standard, *i.e.* H_2O, displays a temperature-dependent $\delta(^{17}O)$ value due to change in the extent of hydrogen bonding, thus affecting indirectly the observed $\Delta\delta O$ values. This problem was probed by measuring the ^{17}O NMR spectra of the non-hydrogen bonding 1,4-dioxane with D_2O standard in an external capillary at 30, 50, 70 and 90 °C. We assumed that the $\gamma(^{17}O)$ value of 1,4-dioxane is temperature insensitive and hence, that the differences reflect a shift of $\delta(D_2{}^{17}O)$. A linear correlation between the relative $\delta(^{17}O)$ shift of 1,4-dioxane *vs.* D_2O with the temperature (not shown) was observed. Interpolation of the differences (6.5 at 90, 3 ppm at 30 °C), suggest a $\delta(^{17}O)$ shift of *ca.* 2 ppm of the standard between 50 and 80 °C. Since this value is much lower than the $\Delta\delta O$ values given above, we conclude that the values are not due to a temperature-dependent shift.

^{13}C *Chemical Shifts* (i) *in* $CDCl_3$.—For group (*i*) enols δ(C-1) = 144–147.2 and δ(C-2) = 110.9–115.6. The $\delta(^{13}C\text{-}1)$ values of **1a** and **c** are almost identical, whereas $\delta(^{13}C\text{-}2)$ for **1a** is at 2.31 ppm lower than for **1c**. Both $\delta(^{13}C\text{-}1)$ and $\delta(^{13}C\text{-}2)$ values for **1b** and **d** are at a lower field than for **c**: by 3.09 and 1.75 ppm for **1b** and by 1.05 and 2.36 ppm for **1d**.

For group (*ii*) δ(C-1) = 148.9–150.3 and δ(C-2) = 110.3–113.5. The latter values correlate with Hammett's δ values (slope = 3.6; R = 0.978). This behaviour resembles that of the analogous β,β-dimethylstyrenes for which ρ = 5.4 (R = 0.991)[17] and *E*-stilbenes.[18,19] A plot of $\delta(^{13}C\text{-}2)$ for group (*ii*) *vs.* $\delta(^{13}C\text{-}2)$ for β,β-dimethylstyrenes[17] is linear (slope = 0.79; R = 0.999).

For group (*iii*) $\delta(^{13}C\text{-}1)$ = 147.3–156.7, $\delta(^{13}C\text{-}2)$ = 108.1–114.7. The $\delta(^{13}C\text{-}1)$ and $\delta(^{13}C\text{-}2)$ SCS values are affected in opposite ways. A change from α-H (**1c** and **d**) to α-Bu^t (**1i** and **j**) β,β-diarylethenol increases $\delta(^{13}C\text{-}1)$ by 10.9–12.6 and decreases $\delta(^{13}C\text{-}2)$ by 4.4–5.0. These changes are less than half of the corresponding changes in $\delta(^{13}C\text{-}1)$ (+26) and $\delta(^{13}C\text{-}2)$ (−15) from ethylene to *tert*-butylethylene.[20a] With the β,β-dimesityl derivatives the change α-H (**1c**) ⟶ α-Mes (**1l**) increases $\delta(^{13}C\text{-}1)$ by 4.6 and $\delta(^{13}C\text{-}2)$ by 1.2.

A $\delta(^{13}C\text{-}1)$ *vs.* $\delta(^{13}C\text{-}2)$ plot for all the enols showed an extensive scatter and R = 0.885 even after excluding the four most deviating points for **1a**, **c**, **i** and **j**.

Replacing a β-mesityl *trans* to the OH in trimesitylethenol (**1l**) by a β-phenyl in *Z*-1,2-dimesityl-2-phenylethenol (**1k**) increases $\delta(^{13}C\text{-}2)$ by 0.25 and $\delta(^{13}C\text{-}1)$ by 1.37.

Most $\delta(^{17}O)$ and $\delta(^{13}C)$ values change roughly in a similar way. An approximate correlation [Fig. 1(*a*)] exists between $\delta(^{17}O)$ and $\delta(^{13}C\text{-}1)$ for the ten enols **1a–j** with strong positive deviation for the α-mesityl derivatives **1k** and **l** (slope = 2.0; R = 0.913). The correlation improves (R = 0.951) for the nine enols **1a**,**c–j** and for **1c–j** the slope is 1.58 (R = 0.953). The $\delta(^{17}O)$ *vs.* $\delta(^{13}C\text{-}2)$ plot [Fig. 1(*b*)] shows much larger scatter although the trend indicates a negative slope.

(ii) *In* $[^2H_6]$*DMSO*. The ^{13}C shifts were also measured in $[^2H_6]$DMSO at 30 °C. The data are given in Table 1 together with the $\Delta\delta C = \delta(^{13}C)([^2H_6]DMSO) - \delta(^{13}C)(CDCl_3)$ values for both C-1 and C-2. All the $\Delta\delta$C-1 values are positive except for −0.10 for **1j**, whereas the $\Delta\delta$C-2 values are negative except small and positive values for **1f**, **h** and **i**, *i.e.*, the changes in $\Delta\delta$C-1 and $\Delta\delta$C-2 are mostly in opposite directions. A plot of $\delta(^{13}C\text{-}1)$ in $CDCl_3$ *vs.* $\delta(^{13}C\text{-}1)$ in $[^2H_6]$DMSO is linear (slope 0.93, R = 0.9845) with a deviation only for **1b** [Fig. 2(*a*)]. A similar plot of $\delta(^{13}C\text{-}2)$ shows an approximate similar trend, with a large scatter. However, two nearly parallel lines (slopes: 0.92 and 0.96, R = 0.9875 and 0.9958, respectively) can be observed for enols **1a–d** and for **1e–j** with points for **1k** and **l** between the two lines [Fig. 2(*b*)]. For PhOH, $\delta(^{13}C_{ipso})$ = 157.23 and $\delta(^{13}C_{ortho})$ = 115.17.

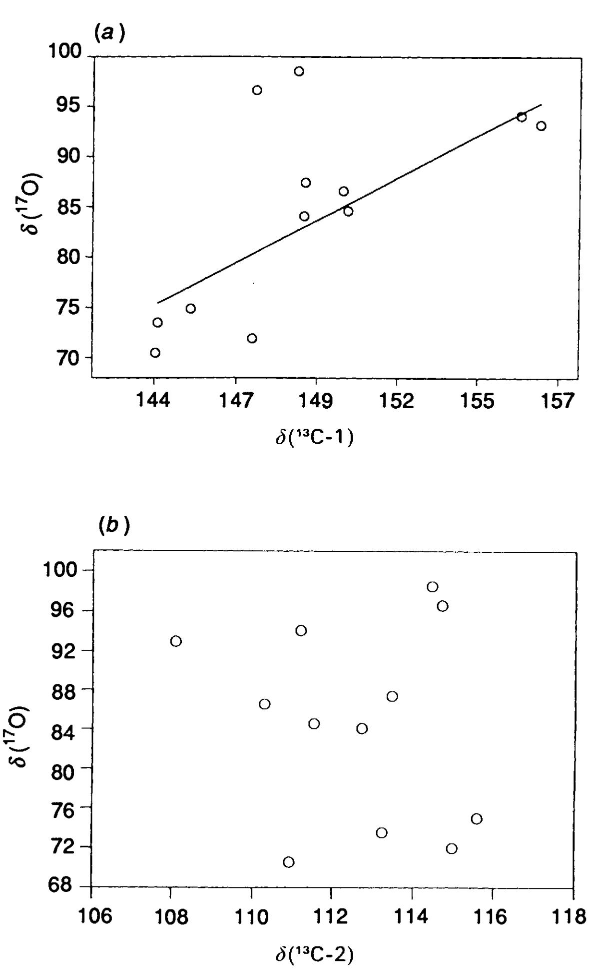

Fig. 1 (*a*) Plot of $\delta(^{17}O)$ *vs.* $\delta(^{13}C\text{-}1)$ in $CDCl_3$. (*b*) Plot of $\delta(^{17}O)$ *vs.* $\delta(^{13}C\text{-}2)$ in $CDCl_3$.

^1H *NMR*.—Previous $\delta(^1H)$ values for the enolic hydrogen in $CDCl_3$ and $[^2H_6]$DMSO and a new value for **1e** in $[^2H_6]$DMSO are given in Table 1. Several of the values were used previously for evaluating the extent of association with DMSO.[4,5] A plot of $\delta(^{17}O)$ *vs.* $\delta(^1HO)$ values both in $CDCl_3$ resembles the $\delta(^{17}O)$ *vs.* $\delta(^{13}C\text{-}1)$ plot. A plot of $\delta(^{17}O)$ in $CDCl_3$ *vs.* $\delta(^1HO)$ in $[^2H_6]$-DMSO is scattered, and excluding the points for **1a**, **k** and **l**, leads to a very approximate linear correlation (slope = −8; R = 0.898). However, for five of the six enols (**1l** excluded) a plot of $\delta(^{17}O)$ values *vs.* $\delta(^1HO)$ values, both in $[^2H_6]$DMSO, is reasonably linear (slope = −6.5; R = 0.963). A plot of $\delta(^{13}C\text{-}1)$ *vs.* $\delta(HO)$ is non-linear and the points concentrate in three regions.

UV Maxima.—Since the longest n ⟶ π* may correlate with $\delta(^{17}O)$, UV spectra of four enols, representatives of the three groups were measured in $CDCl_3$ and those for **1f** and **l** also in hexane, in which λ_{max} for **1c**, **b** and **i** were previously reported.[3a,14] (Table 1). The spectra for **1f** and **l** have Gaussian shape, but those for **1c** and **l** display a lower intensity, higher wavelength unresolved shoulder, superimposed on the main absorption, so that the longest wavelength (probably π ⟶ π*)

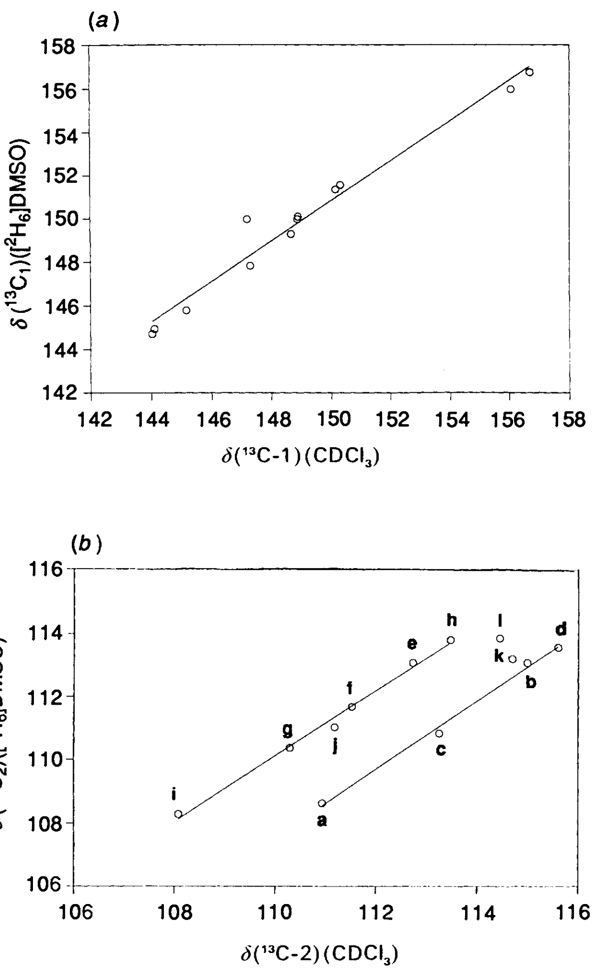

Fig. 2 Plots of $\delta(^{13}C)$ values in $[^2H_6]$DMSO *vs.* those in $CDCl_3$; (*a*) for C-1; (*b*) for C-2; letters relate to enols **1**

λ_{max} may be hidden. Other λ_{max} values (in nm) in hexane are **1c**, 227; **1f**, 217, 245; **1i**, 231 and **1l**, 215, 238.

Calculated Charge Densities by the PM3 Method.—The charge densities, q, and the heats of formation ΔH_f for the four representative enols **1c**, **f**, **i** and **l** were calculated by the PM3 method by changing the C-2–C-1–O–H torsional angle θ, from its value at the *syn* (*s*) conformation ($\theta = 0°$) to the *anti* (*a*) conformation ($\theta = 180°$) in steps of 30° in both directions. The calculated qs at C-1, C-2, O and H and the ΔH_f values are given in Table 2 and representative plots against θ for **1c** and **l** are shown in Figs. 3 and 4. The following features are important:

(*i*) The enol structure affects only slightly the calculated charge density at O [-0.216–-0.023 (*a*), -0.238–-0.249 (*s*)] and at C-2 [-0.075–-0.089 (*a*), -0.143–-0.159 (*s*)] and H [0.188–0.198 (*a*) and 0.205–0.210 (*s*)] and more so at C-1 [0.005–0.099 (*a*), 0.051–0.139 (*s*)]. However, the difference in charge densities between $\theta = 0$ and 90° are structure dependent, being 0.021 (**1c**) > 0.020 (**1i**) > 0.013 (**1f**) > 0.008 (**1l**).

(*ii*) All the ΔH_f values are negative, except those for **1f**, at θ = 60–180° and -90–$-180°$. The decrease of ΔH_f from **1l** to **f** on reduced methylation is reminiscent of the ΔH_f values of benzene and toluene.

(*iii*) The *syn* conformations **1c**(*s*), **1f**(*s*), **1i**(*s*) and **1l**(*s*) are the most stable, having more negative ΔH_f values. These values increase with θ until a maximum value is reached at the perpendicular conformations **1c**(p), **1f**(p), **1i**(p) and **1l**(p) or at $\theta = 120°$, and then decrease further on approaching the *anti* conformations **1c**(*a*), **1f**(*a*), **1i**(*a*) and **1l**(*a*). The change is more pronounced for **1c**, where $\Delta H_f[\mathbf{1c}(s)] - \Delta H_f[\mathbf{1c}(a)] = -5.3$ kcal mol^{-1} and $\Delta H_f[\mathbf{1c}(s)] - \Delta H_f[\mathbf{1c}(p)]$ = *ca.* -6 kcal mol^{-1} than for **1f**, **i** and **l**.

Table 2 ΔH_f (kcal mol^{-1}) and charge densities q at the atoms of the $C_2{=}C_1{-}O{-}H$ moiety at different θ values

θ	ΔH_f	q(C-2)	q(C-1)	q(O)	q(H)
For **1c**					
180	-26.1	-0.089	0.005	-0.216	0.188
150	-25.6	-0.078	0.001	-0.227	0.190
120	-25.0	-0.058	0.005	-0.247	0.194
90	-25.2	-0.059	0.001	-0.259	0.195
60	-27.2	-0.094	0.017	-0.253	0.200
30	-30.0	-0.138	0.039	-0.241	0.203
0	-31.4	-0.159	0.051	-0.238	0.205
-30	-31.1	-0.145	0.045	-0.248	0.209
-60	-29.0	-0.104	0.023	-0.260	0.207
-90	-26.7	-0.065	0.001	-0.264	0.202
-120	-25.4	-0.058	-0.006	-0.247	0.194
-150	-25.9	-0.077	0.005	-0.227	0.189
For **1f**					
180	1.82	-0.075	0.086	-0.225	0.196
150	1.86	-0.060	0.077	-0.232	0.196
120	2.88	-0.038	0.067	-0.244	0.196
90	3.28	-0.041	0.069	-0.249	0.196
60	2.00	-0.078	0.088	-0.244	0.199
30	-0.24	-0.123	0.112	-0.236	0.204
0	-1.38	-0.143	0.125	-0.236	0.208
-30	-0.73	-0.124	0.118	-0.248	0.212
-60	-0.34	-0.083	0.096	-0.259	0.210
-90	1.35	-0.047	0.076	-0.258	0.204
-120	1.96	-0.042	0.073	-0.241	0.196
-150	1.30	-0.063	0.082	-0.225	0.195
For **1i**					
180	-43.9	-0.089	0.052	-0.238	0.198
150	-44.4	-0.079	0.050	-0.241	0.197
120	-43.4	-0.056	0.041	-0.255	0.198
90	-43.5	-0.056	0.044	-0.269	0.203
60	-44.3	-0.092	0.065	-0.270	0.209
30	-45.4	-0.139	0.089	-0.255	0.210
0	-46.1	-0.159	0.088	-0.249	0.210
-30	-45.0	-0.140	0.086	-0.249	0.206
-60	-42.9	-0.095	0.059	-0.257	0.201
-90	-41.5	-0.053	0.037	-0.264	0.198
-120	-42.0	-0.048	0.032	-0.261	0.200
-150	-43.3	-0.070	0.042	-0.249	0.199
For **1l**					
180	-22.7	-0.078	0.099	-0.234	0.198
150	-22.8	-0.064	0.092	-0.247	0.203
120	-22.0	-0.042	0.081	-0.260	0.202
90	-20.8	-0.079	0.081	-0.251	0.199
60	-21.9	-0.124	0.100	-0.243	0.199
30	-24.0	-0.124	0.125	-0.243	0.203
0	-24.9	-0.145	0.139	-0.243	0.208
-30	-24.2	-0.127	0.132	-0.254	0.211
-60	-23.1	-0.085	0.109	-0.265	0.209
-90	-22.2	-0.049	0.088	-0.266	0.204
-120	-21.7	-0.044	0.084	-0.250	0.197
-150	-22.5	-0.065	0.094	-0.236	0.196

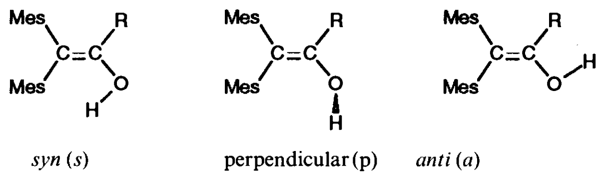

syn (*s*)	perpendicular (p)	*anti* (*a*)
1c (*s*):R = H	**1c** (p):R = H	**1c** (*a*):R = H
1f (*s*):R = Ph	**1f** (p):R = Ph	**1f** (*a*):R = Ph
1i (*s*):R = Bu^t	**1i** (p):R = Bu^t	**1i** (*a*):R = Bu^t
1l (*s*):R = Mes	**1l** (p):R = Mes	**1l** (*a*):R = Mes

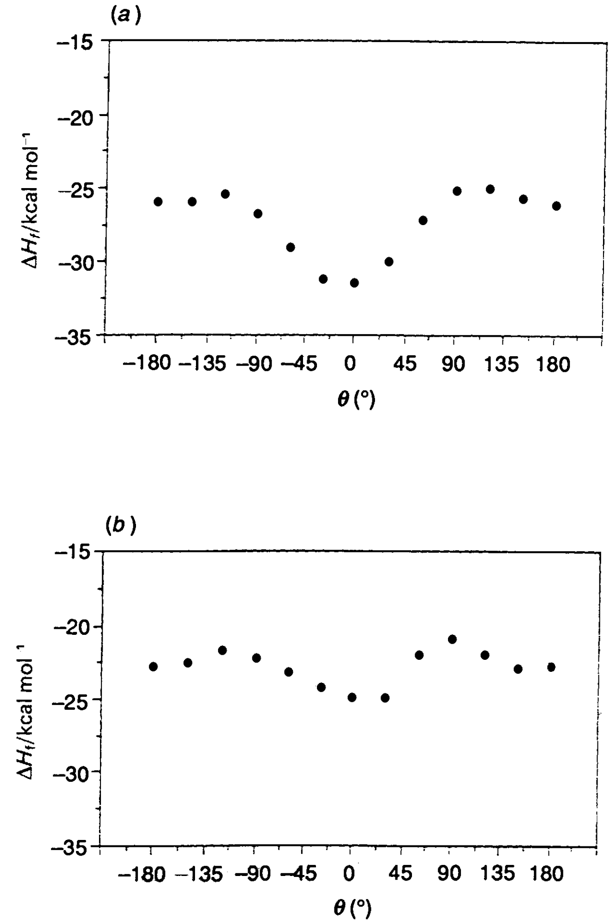

Fig. 3 Calculated ΔH_f (kcal mol^{-1}) values (by PM3) for **1c** (*a*) and **1l** (*b*) *vs.* the torsional angle θ

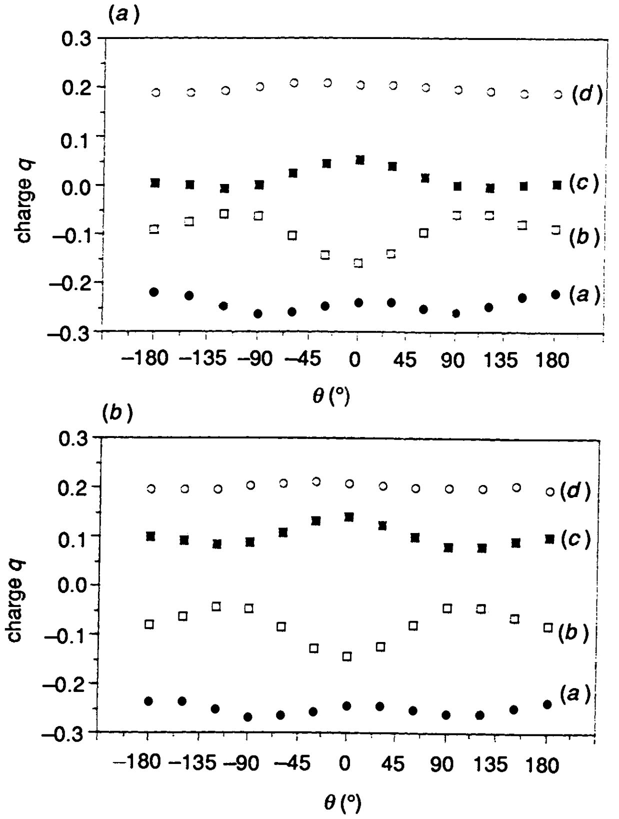

Fig. 4 Calculated charge densities q (by PM3) for the four atoms of the C-2=C-1–O–H moiety of (*a*) **1c** and (*b*) **1l** *vs.* the torsional angle θ; (*a*) (●), O; (*b*) (□), C-2; (*c*) (■), C-1; (*d*), (○), H

(*iv*) The ΔH_f values for θ and $-\theta$ are different, *e.g.*, −1.5 to −2.0 kcal mol^{-1} for $\theta = -90$ and $\theta = 90°$ for the (p) conformation.

(*v*) C-2 and O are always negative and H and C-1 are always positive except for a single slightly negative value for C-1 at θ = 120° for **1c**. The largest absolute charges are for C-2, where q is nearly twice the value for the (*s*) than for the (*a*) conformation and the smallest for the H. The q values at θ = 0° are the most negative for C-2, the most positive for C-1 and the least negative for O, while they are the most positive for H at θ = 0–30°. A maximum for C-2 appears at the θ = 90—120°. The q values are again unequal for θ and $-\theta$ values.

(*vi*) Fig. 4 shows that the changes are larger for C-2 and C-1, that the shapes of q *vs.* θ plots for them are approximately mirror images of one another and that the effect of change in θ on O and H is smaller.

If a reciprocal relationship exists between δ and q values, the highest field ^{13}C-2 and the lowest field ^{17}O shift values are predicted for the (*s*) conformations, the lowest field ^{13}C-2 and the highest field ^{17}O shifts for the (p) conformations and $\delta(^{13}\text{C-2})[a] > \delta(^{13}\text{C-2})[s]$ for all enols. The effect on $\delta(^{13}\text{C-1})$ and $\delta(^{17}\text{O})$ values will be smaller.

Table 3 Calculated absolute energies (Hartrees) of ethenol and propen-2-ol in three principal conformations

		Conformation		
	Method	*syn* (*a*)	per (*b*)	*anti* (*c*)
Ethanol (**4**)	HF/6-31G**	−152.9010	−152.8939	−152.8977
	HF/6-311G**	−152.9379	−152.9306	−152.9347
	MP2/6-311G**	−153.4226	−153.4138	−153.4193
Propen-2-ol (**5**)	MP2/6-311G**	−192.6260	−192.6170	−192.6220

IGLO Calculations.—Since the δ values cannot be calculated for our stable enols by *ab initio* methods, the $\delta(^{17}\text{O})$, $\delta(^{13}\text{C})$ and the $\delta(^{1}\text{H})$ values for an isolated molecule were calculated by the IGLO method using the basis II′ and geometries optimized at MP2/6-311G** level of theory (IGLO/basis II′//MP2/6-311G**) for the simplest enols, vinyl alcohol **4** and propen-2-ol **5**. The geometry optimizations have been carried out for structures with C=C–O–H torsion angles (θ), which were changed at 10° intervals from 0 to 180°. For **5**, only the three extreme conformations, the *cis*-periplanar (**5a**), θ = 0°; the perpendicular (**5b**), θ = 90° and the *anti*-periplanar conformation (**5c**), θ = 180° were calculated. The calculated absolute energies of **4** and **5** at the three conformations are given in Table 3, the calculated shifts are given in Table 4 and the structures and charge densities of **4a**, **b** and **c** calculated at HF/6-31G** are shown in Fig. 5. The geometry parameters of the C=C–OH moiety in the three conformations are very similar except for a calculated longer C–O bond in **4b**. A plot of the relative energy *vs.* θ is given in Fig. 6, which resembles Fig. 3 in its general appearance.

The IGLO/basis II′ calculations do not reproduce the reported experimental $\delta(^{13}\text{C})$ chemical shifts of **4** and **5**.[6] Using the recently developed MBPT(2) version of the GIAO method for calculating NMR chemical shifts, we recalculated with a considerable larger basis set [*qzp*(C,O)/*tzp*(H)] the chemical shifts of the three principal conformations of **4** using the same MP2/6-311G** optimized geometries. The MBPT(2)/GIAO calculated chemical shifts of **4a–c** (Fig. 7) reproduce in a satisfactory manner the experimental ^{13}C chemical shifts. However, since the major differences between the calculated

Table 4 Calculated $\delta(^{17}O)$, $\delta(^{13}C)$ and $\delta(^{1}H)$ values and charges q (Mulliken population analysis) at O, C and H for three extreme conformations of ethenol **4** with and without added $H_2S{=}O$, at various levels and geometries [see (*a*)–(*d*)] and of enol **5a**

Compound/ Conformation	$\delta(^{17}O)^a$	$\delta(^{13}C\text{-}1)^b$	$\delta(^{13}C\text{-}2)^b$	$\delta(^{1}H)^b$	q(O)	q(C-1)	q(C-2)	q(H)
(*a*) δ At IGLO/Basis II′//MP2/6-311G**, at dielectric constant 1. Charges at MP2/6-311G**								
4a	82.7	175.8	105.2	4.66	−0.41	+0.15	−0.33	+0.26
4b	48.4	174.6	129.8	2.95	−0.44	+0.08	−0.24	+0.26
4c	78.5	172.5	112.8	3.80	−0.41	+0.12	−0.29	+0.26
5a	91.5	186.7	100.8	4.94	−0.45	+0.15	−0.30	+0.26
5b	61.5	185.1	122.7	3.03	−0.48	+0.10	−0.23	+0.26
5c	81.2	180.9	105.2	3.43	−0.44	+0.16	−0.28	+0.25
(*b*) δ At IGLO/Basis II′//HF/6-311G**, [c] at dielectric constant 1. Charges at HF/6-311G**								
4a	68.5	170.3	100.8	3.84	−0.41	+0.15	−0.33	+0.25
4b	37.2	169.0	124.4	2.28	−0.44	+0.09	−0.24	+0.26
4c	66.6	166.6	107.0	3.13	−0.41	+0.13	−0.29	+0.26
(*c*) δ At IGLO/Basis II′//SCRF/HF/6-311G**, at dielectric constants 4.8 (46.7). Charges at HF/6-311G**								
4a	68.7 (68.7)	170.1 (170.1)	100.8 (100.8)	3.88 (3.88)	−0.41 (−0.42)	+0.15 (+0.15)	−0.32 (−0.32)	+0.26 (0.26)
4b	37.5 (37.6)	168.7 (168.9)	124.4 (124.4)	2.28 (2.27)	−0.45 (−0.45)	+0.09 (+0.09)	−0.24 (−0.24)	+0.27 (0.27)
4c	66.8 (66.9)	166.7 (166.7)	107.0 (107.0)	3.15 (3.16)	−0.42 (−0.42)	+0.14 (+0.14)	−0.30 (−0.30)	+0.26 (0.27)
(*d*) δ At IGLO/Basis II′//HF/6-31G** for different degrees of complexation. Charges at HF/6-31G**								
4a	69.4	170.2	100.9	4.0	−0.61	+0.25	−0.39	+0.35
4a·O=SH$_2$(C_1)[d]	63.0 (54.1)	173.2 (170.1)	97.9 (100.8)	7.2 (6.9)	−0.65 (−0.67)	+0.25 (0.26)	−0.42 (−0.39)	+0.40 (0.40)
Δ[e]	−6.4 (−15.3)	+3.0 (−0.1)	−3.0 (−0.1)	3.2 (2.9)				
4a·O=SH$_2$(C_1, SCRF)[f]	60.4	171.2	98.7	7.2	−0.65	+0.27	−0.40	+0.41
Δ[g]	−9	+1.0	−2.2	3.2				
4b	37.9	168.8	124.5	2.4	−0.63	+0.21	−0.32	+0.35
4b·O=SH$_2$	21.9	169.4	122.3	5.5	−0.69	+0.23	−0.33	+0.40
Δ[e]	−16.0	0.6	−2.2	3.1				
4b·O=SH$_2$(C_1, SCRF)[f]	37.7	172.6	119.5	5.5	−0.69	+0.22	−0.34	+0.41
Δ[g]	−0.2	3.8	−5.0	3.1				
4c	67.4	166.6	107.0	3.2	−0.61	+0.22	−0.35	+0.35
4c·O=SH$_2$(C_1)[d]	51.4 (55.5)	168.6 (168.6)	103.9 (103.5)	6.6 (6.5)	−0.66 (−0.67)	+0.23 (0.24)	−0.37 (−0.37)	+0.40 (0.40)
Δ[e]	−16 (−11.9)	2.0 (2.0)	−3.1 (−3.5)	3.4 (3.3)				
4c·O=SH$_2$(C_1, SCRF)[f]	65.7	171.1	100.6	6.6	−0.64	+0.27	−0.40	+0.41
Δ′[g]	−1.7	4.5	−6.4	3.4				

[a] $\delta(H_2{}^{17}O) = 0$. [b] $\delta(\text{TMS}) = 0$. [c] $\delta(^{13}C)$ are almost the same and $\delta(^{17}O)$ values are 0.7–0.9 ppm higher at IGLO/Basis II′//HF/6-31G**. In medium with a dielectric constant of 46.7, the shifts differ by ≤0.4 ppm. [d] Values for the complex with C_s symmetry are given in parentheses. [e] Δ = δ(**4**·O=SH$_2$) − δ(**4**). [f] In medium with a dielectric constant of 46.7. [g] Δ′ = δ[**4**·O=SH$_2$(C_1, SCRF)] − δ(**4**).

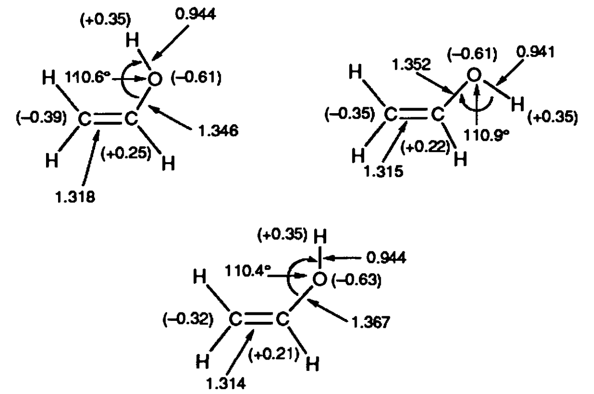

Fig. 5 Calculated structures (HF/6-31G**) and Mulliken charge densities (in parentheses) [HF/6-31G**] for **4a**, **4b** and **4c**

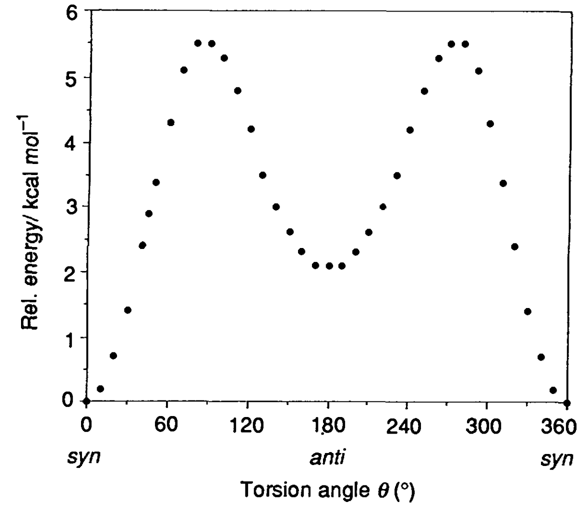

Fig. 6 A plot of relative energies (MP2/6-311G**, kcal mol^{-1}) *vs.* the torsional angle θ for **4**

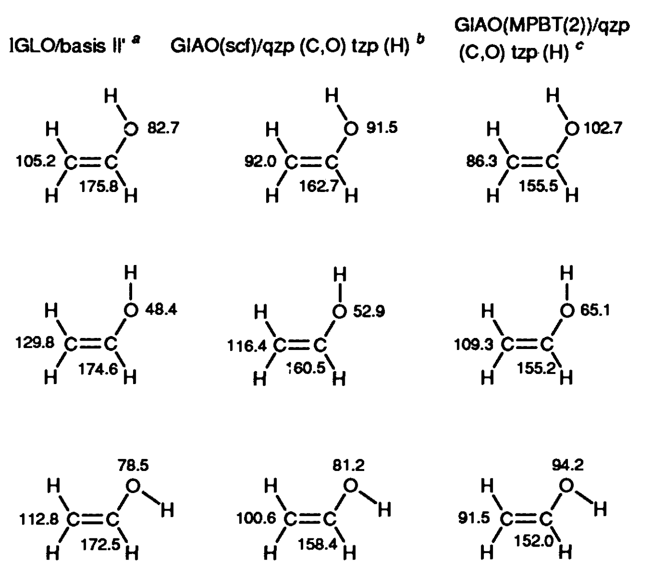

Fig. 7 Comparison of δ(^{17}O) and δ(^{13}C) values calculated by IGLO and the higher level GIAO [MPBT(2)] methods. [a] δ(^{13}C, TMS) = 0, calculated chemical shielding σ(^{13}C) = 213.28 ppm (IGLO/basis II'//HF/6-31G*), δ(^{17}O, H_2O) = 0, calculated chemical shielding σ(^{17}O) = 292.81 ppm (IGLO/basis II'//HF/6-31G*). [b] δ(^{13}C, TMS) = 0, calculated chemical shielding σ(^{13}C) = 193.42 ppm (GIAO/SCF/tzp/dzp//MP2/6-31G*), δ(^{17}O, H_2O) = 0, calculated chemical shielding σ(^{17}O) = 324.8 ppm (GIAO/SCF/qzp/tzp//MP2/6-31G*). [c] δ(^{13}C, TMS) = 0, calculated chemical shielding σ(^{13}C) = 197.19 ppm (GIAO/MBPT(2)/tzp/dzp//MP(2)/6-31G*), δ(^{17}O, H_2O) = 0, calculated chemical shielding σ(^{17}O) = 342.8 ppm (GIAO/MBPT(2)/qzp/tzp//MP2/6-31G*).

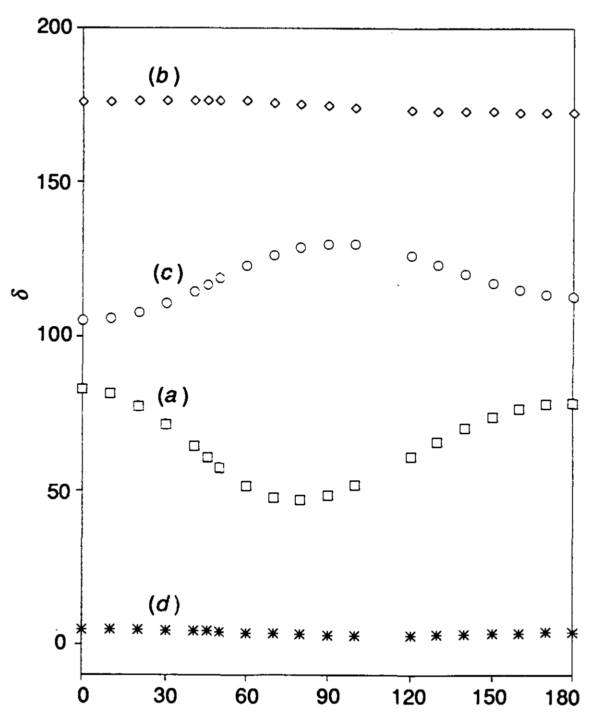

Fig. 8 Calculated [by IGLO/Basis II'//MP2/6-311G**] ^{17}O, ^{13}C and ^{1}H chemical shifts for **4** *vs.* the torsional angle θ: (*a*) δ(^{17}O); (*b*) δ(^{13}C-1); (*c*) δ(^{13}C-2); (*d*) δ(^{1}H)

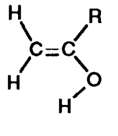

4a R = H
5a R = Me

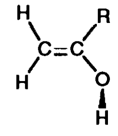

4b R = H
5b R = Me

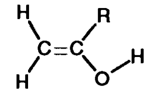

4c R = H
5c R = Me

chemical shifts of the principal conformations of **4** are already present to the same extent in the IGLO results, we used the computationally cheaper IGLO method throughout.

The plots of δ *vs.* θ (Fig. 8) show that δ(^{17}O), δ(^{1}H) and δ(^{13}C-2) are more sensitive than δ(^{13}C-1) to the C=C–O–H conformation. The δ(^{17}O) value starts at 82.7 for **4a**, and decreases steadily until it reaches a minimum of 46.9 at θ = 80° and increases again to 78.5 for **4c**, giving a shallow parabola plot for **4**. The δ(^{13}C-2) values show a roughly mirror-image behaviour. From 105.2 ppm for **4a** they increase to 129.8 for **4b** and then decrease to 112.8 at **4c**. δ(^{13}C-1) decreases very slowly and steadily from **4a** to **b** to **c**. The apparent small change in the δ(^{1}H) *vs.* θ plot is misleading since the range of δ(^{1}H) values is much smaller than the δ(^{17}O, ^{13}C) ranges and the relative change is appreciable and parallel to that of δ(^{17}O) (Table 4). The higher value (δ 4.66) is at θ° = 0 and the lowest value at θ = 100° (δ = 2.85). Changes for **5** parallel those of **4** [Table 4(*a*)].

The change in θ reduces the π(C=C)–p(O) interaction but increases the π(C=C)–sp^2(O) interaction with the other oxygen lone pair. We therefore conducted an NBO analysis for **4a**, **b** and **c**. We analysed the second order perturbation energy term ΔEσσ* which is the energy lowering gained by the perturbative donor–acceptor interaction involving a filled σ orbital of the Lewis structure and a formally empty σ* orbital. We found that ΔEσσ* calculated for the π*(C=C)–sp^2(O) interaction in the perpendicular conformation is lower than the ΔEσσ* calculated for the π*(C=C)–p(O) in the *syn* and the *anti* conformers, due to the larger energy difference and lower overlap between the

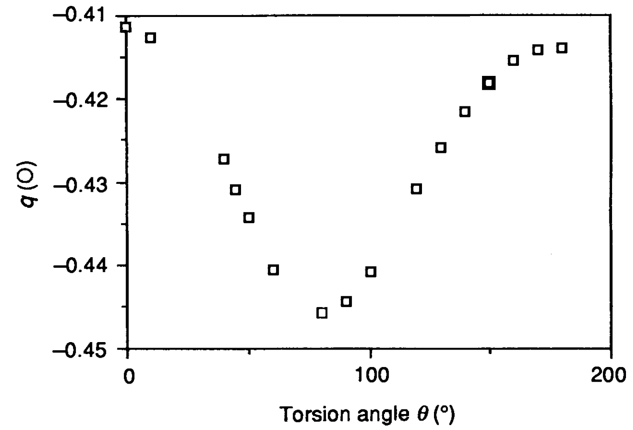

Fig. 9 Plot of the calculated Mulliken charges at the oxygen *vs.* the torsion angle θ

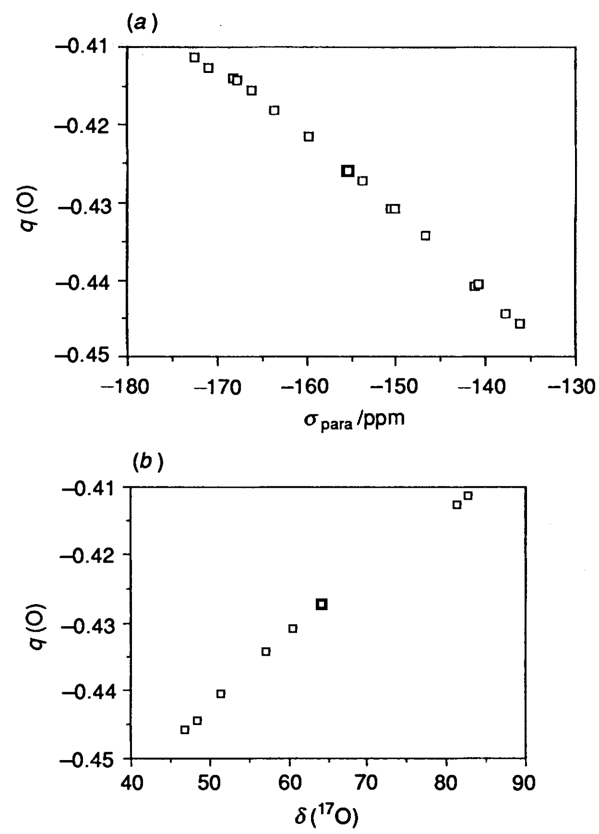

Fig. 10 Plots of the charge on the oxygen *vs.* (*a*): $\sigma_O{}^p$ (ppm) and (*b*): $\delta(^{17}O)$

former than between the latter orbitals. Consequently, the electron density at the oxygen of the perpendicular conformation is larger.

Inspection of the IGLO calculations leads to the following conclusions: (*a*) of the two screening constants which affect ^{17}O chemical shifts only the paramagnetic term $\delta_O{}^p$ changes during the conformational change. The diamagnetic term ($\sigma_O{}^d$) remains nearly constant. (*b*) The dependence of the Mulliken charges at oxygen on the torsional angle θ parallels its dependence on $\delta(^{17}O)$, *i.e.*, the more negative is the oxygen the lower is the $\delta(^{17}O)$ value. The highest negative charge is for the perpendicular conformation (Fig. 9). The increase of the electron density at the oxygen leads to decrease in $|\sigma_O{}^p|$ which in turn leads to a shift of $\delta(^{17}O)$ to a higher field (Fig. 10). (*c*) The $\sigma_O{}^p$ term is reciprocally linear with the 'mean excitation energy', [*cf.* eqn. (1)]. ΔE is expected to change on rotating the OH group from the double bond plane. Instead of calculating the first excited states of all conformers, the HOMO–LUMO energy difference was plotted against $\sigma_O{}^p$, and a reciprocal linear relation was indeed observed (Fig. 11). Consequently, both increased electron density at the oxygen and increased ΔE are responsible for the observed shielding.

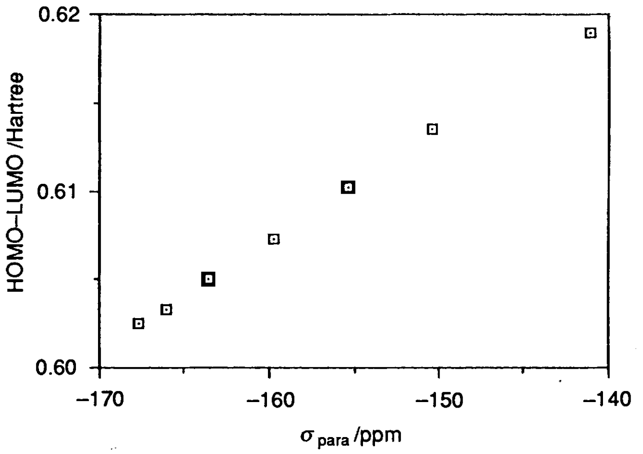

Fig. 11 A plot of the HOMO–LUMO difference *vs.* $\sigma_O{}^p$

Table 5 Calculated absolute energies (E_{abs}) of ethenol complexes with $H_2S{=}O$ (HF/6-31G** and SCRF/6-31G**)[a]

Complex	ε^b	$a_o{}^c$	E_{abs} Hartree	$E_{rel}{}^d$/ kcal mol⁻¹	$E_{ZPE}{}^e$/ kcal mol⁻¹
4a·O=SH$_2$	1	—	−626.3612	0	0
4a·O=SH$_2$	46.7	3.85	−626.3661	0	
4b·O=SH$_2$	1	—	−626.3530	5.1	5.1
4b·O=SH$_2$	46.7	3.86	−626.3598	3.9	
4c·O=SH$_2$	1	—	−626.3585	1.7	1.3
4c·O=SH$_2$	46.7	3.84	−626.3691	−1.9	

[a] E_{abs} ($H_2S{=}O$) = −473.4451 Hartree, ZPE = 14.6 kcal mol⁻¹. [b] Dielectric constant. [c] Cavity radius a_o in Angstroms. [d] Relative energies. [e] Relative energies E_{ZPE} including zero point vibration energy in kcal mol⁻¹.

For evaluating the solvent effect, several types of calculations have been performed. First, geometries of **4** were calculated at the HF/6-311G** level in the gas phase, *i.e.*, for a dielectric constant of 1. By using these geometries the chemical shifts were calculated by the IGLO method. It is noteworthy that all the shifts are at a significantly higher field than at the higher level MP2/6-311G** calculations. Second, the geometry optimizations were then conducted in media having the dielectric constants of $CHCl_3$ (4.8) and DMSO (46.7), modelled using the Self Consistent Reaction Field Theory at the HF/6-311G** level. The effect of the medium is negligible on both the calculated chemical shifts for these structures (≤ 0.4 ppm, mostly ≤ 0.2 ppm) and the charge densities [Table 4(*b*) and (*c*)]. Third, IGLO calculations of the $\sigma(^{17}O, ^{13}C, ^1H)$ shifts for conformations **4a**, **b** and **c** were performed on calculated geometries of **4** and of the 1 : 1 complex of **4** with the sulfoxide $H_2S{=}O$, a model for dimethyl sulfoxide, optimized by using the HF/6-31G** basis.

The geometry optimization for the *syn* and *anti* complexes were performed without any symmetry constraints. In the optimized structures of the *syn* and *anti* complexes the initial value of the C=C–O–H torsion angle remains nearly unchanged on complexation. In the complexes the deviation from perfect *anti*-orientation in the *anti* complex is 1.2° and from ideal *syn*-orientation in the *syn* complex it is 2.2°. In all three conformations the $H_2S{=}O$ molecule is located above the C=C–O-plane. The structures of the complexes are given in Fig. 12(*a*) and the calculated absolute energies are given in Table 5. The complexes **4**·O = SH$_2$ have very flexible geometries. The

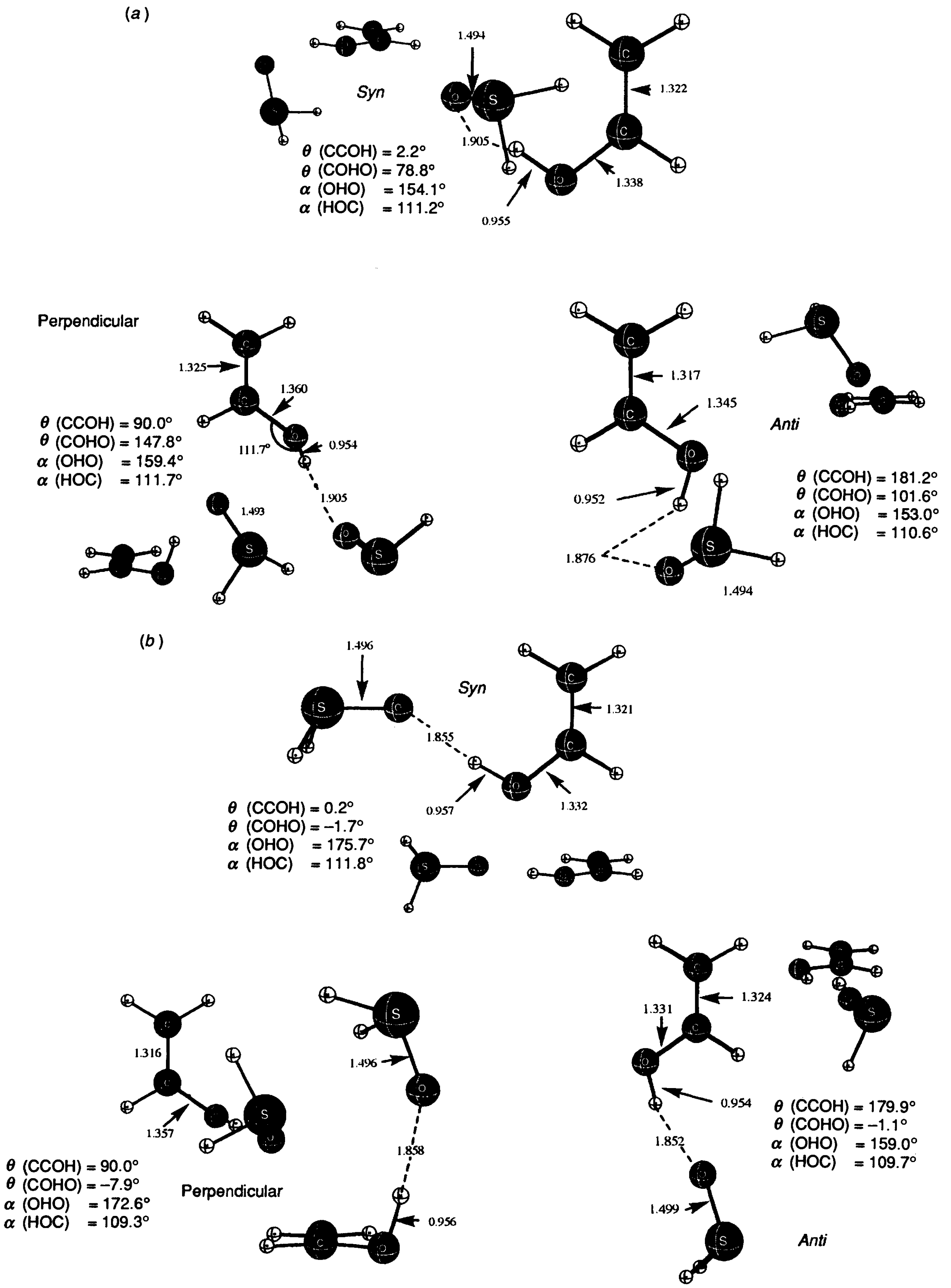

Fig. 12 Calculated structures of $4{\cdot}O{=}SH_2$: (*a*) [RHF/6-31G**], no constraints, C_1 geometry for **4a**, **4b** and **4c**; (*b*) [RHF/6-31G**, SCRF optimization, C_1] at dielectric constant 46.7 for **4a**, **4b** and **4c**

energy difference between the most stable C_1 structures of $\mathbf{4a}{\cdot}O{=}SH_2$ and $\mathbf{4c}{\cdot}O{=}SH_2$ and structures of these complexes which are restricted to C_s symmetry are merely 0.6 and 0.2 kcal mol^{-1}, respectively. The *syn* conformation is 1.3 and 5.1 kcal mol^{-1} more stable than the *anti* and the perpendicular conformation, respectively. The hydrogen bridge is stronger in the *anti* complex by 0.4 and 0.8 kcal mol^{-1} than in the *syn* and perpendicular conformations, respectively. Table 4(*d*) also gives

Table 6 Calculated δ (ppm) values for $H_2C{=}C(OH)Me$ at the *anti* conformation (**5a**)

	$\delta(^{17}O)$	$\delta(^{13}C\text{-}1)$	$\delta(^{13}C\text{-}2)$	$\delta(^{1}HO)$
5a, [IGLO/Basis II′//MP2/6-311G**]	81.2	180.9	105.2	3.43
[IGLO/Basis II′//3-31G**]	84.1	176.3	102.1	3.15
5a·$H_2S{=}O$				
[IGLO/Basis II′//6-31G** (C_1)]	64.2	179.0	99.6	6.40
[IGLO/Basis II′//SCRF/6-31G** (C_s)]	86.3	184.5	102.6	6.71
Δ^a	+2.2	+8.2	+0.5	3.56

[a] Δ = δ(IGLO/Basis II′//SCRF/6-31G** (C_s)) − δ(IGLO/Basis II′/6-31G**) values.

the calculated shifts for both geometries and the differences Δ between the shifts of the non-complexed and complexed **4**. Appreciable differences in δs for **4** are found going from an isolated molecule of **4** to the 1:1 complex **4**·$O{=}SH_2$. The calculated $\delta(^{17}O)$ values in the complexes are at a higher field than in the three corresponding non-complexed conformations. The differences are −16 ppm in the perpendicular and *anti* conformations and −6.4 in the *syn* conformation. $\delta(^{13}C\text{-}1)$ is downfield and $\delta(^{13}C\text{-}2)$ is upfield in all conformations of the complexed enol and the hydroxy hydrogen is strongly deshielded by *ca.* 3 ppm.

Reoptimization of the calculated structures in the presence of a reaction field with a dielectric constant $\varepsilon = 46.7$ leads to SCRF calculated structures with nearly C_s symmetry for the *syn* and *anti* conformations [Fig. 12(*b*)]. There are significant changes in the structure of the complexes compared with their calculated gas phase structures, and the C–O (1.331 Å) and the $H_2S{=}O \cdots H$ (1.85 Å) bonds become shorter. The C–O bond of the perpendicular conformation is 0.025 Å longer than in the other conformations.

The derived IGLO/basis II′ calculated chemical shifts based on these optimized geometries are given in Table 4(*d*), together with the $\Delta' = \delta(\mathbf{4}{\cdot}O{=}SH_2) - \delta(\mathbf{4})$ values. The oxygen is still more shielded than in the corresponding non-complexed conformation **4**, but the differences, *i.e.*, −9, −0.2 and −1.7 ppm for the *syn*, perpendicular and *anti* conformations, respectively, are not large. The Δ′ values are positive for C-1 and H and are negative for C-2 for all conformations.

Finally, in order to see whether this behaviour applies also for an α-substituted vinyl alcohol, IGLO calculations were performed for the propen-2-ol complex with $H_2S{=}O$, *i.e.*, **5**·$O{=}SH_2$ with and without self consistent reaction field. For the SCRF calculations the geometry optimization was restricted to the *anti* conformer and to C_s symmetry. The data in Table 6 indicate that all the four signals are calculated to be shifted downfield, with the lowest effects for $\delta(^{17}O)$ and $\delta(^{13}C\text{-}2)$.

Discussion

^{17}O *Chemical Shifts.*—^{17}O shifts are usually analysed in terms of the effects of various parameters on the paramagnetic shielding $\sigma_O{}^p$ of the Karplus–Pople equation [eqn. (1)].[21] ΔE is

$$\sigma_O{}^p = -\text{Const.}\ \Delta E^{-1}\cdot(r^{-3})_{2p_O}\Sigma Q \qquad (1)$$

the electronic excitation energy, approximated by the energy of the lowest energy λ_{max} in the UV–VIS spectrum, r is the radius of the oxygen 2p orbital and Q is the charge density bond order matrix. Alternatively, observed effects such as torsion angle, resonance, polar, steric and hydrogen bonding effects which affect the terms of eqn. (1) by changing electron density at oxygen are independently discussed, as we will do here.

The sub-division to three groups based on $\delta(^{17}O)$ values in $CDCl_3$ depends on the enols studied and the solvent. The question arises as to how representative is the group of enols investigated. One justification of our choice is that enols **1a–l** constitute a significant fraction of all the known stable simple aryl-substituted enols[2] and they represent the main structural features known, *i.e.*, increased bulk at C-2 and small and large substituents at C-1. The conformation of all the enols in $CDCl_3$ is presumably similar, being *syn*-periplanar.[4,5] This division seems related to the bulk of R. The lower $\delta(^{17}O)$ values are for group (*i*) with the smallest α-H-substituent; group (*ii*) have a larger R = *o*-unsubstituted aryl and group (*iii*) included the most bulky, α-Bu^t and α-Mes groups. The difference in the $\delta(^{17}O)$ values is smaller than for ArCOMe [*e.g.*, $\delta(^{17}O)$ = 552, 601 and 607 for Ar = Ph, Mes, Tip, respectively),[22] and higher than the effect of *o*-Me substituents on $\delta(^{17}C{=}O)$ values of $ArCO_2Me$.[23]

Changes in the latter systems are ascribed to changes in the Ar–C=O torsion angle. However, deshielding on increasing steric hindrance is also found in the rigid *o,o′*-disubstituted anisoles[24] or 2-alkylpyridine *N*-oxides, where 'compressional effects' or 'disruption of solvent structure' were invoked.[25] It was noted both that ^{17}O NMR is a powerful method for detection of steric effects in organic systems and that the origin of the steric factors that affect ^{17}O NMR data is still unclear.[8a,b]

Comparison with Other Systems.—Since this is the first work on $\delta(^{17}O)$ values of simple stable enols comparison with systems containing structural elements present in the enols is worthwhile.

Relevant $\delta(^{17}O)$ values are for the intramolecularly hydrogen bonded enols $RC(OH){=}CHCO_2Et$; $\delta(^{17}O)$ = 96.0–124.0,[12] values mostly higher than for enols **1**. The values are higher when R = Me than for R = Ph, CF_3.

Aliphatic alcohols display ^{17}O signals at −37.0 (MeOH) to 62.3 ppm (Bu^tOH) and the SCS may reflect polarization in the sense $^{\delta-}O\text{-}H^{+\delta}$.[13] In RCH_2OH $\delta(^{17}O)$ increases by 30 ppm from R = H to R = Bu^t. Since MeOH and Bu^tCH_2OH are the saturated analogs at C-1 of enols **1c** and **i** or **1d** and **j**, replacing two hydrogens in MeOH by a β-$Ar^1Ar^2C{=}$ moiety results in extensive deshielding. The change of 30 ppm is in the same direction but 50% larger than that for **1d** ⟶ **j**. Consequently, the change in $\delta(^{17}O)$ from a group (*i*) α-H to a group (*iii*) α-Bu^t substituent can be *mainly* due to an electronic effect.

Benzyl alcohols are the C-1 analogs of group (*ii*) enols and **1k** and **l**. Their shifts are geometry-dependent.[26] At a constant geometry *p*-electron-attracting (donating) substituents caused upfield (downfield) shift of the $\delta(^{17}O)$ values.[27] The normal trend of the $\delta(^{17}O)$ SCS in acetone (*p*-CF_3 < H < *p*-MeO) was not found for **1e–h** where the point for *p*-CF_3 seems to deviate. An unusual effect of *p*-CF_3 was noted in ^{13}C NMR spectra.[28]

Our work supplements the data for crowded benzyl alcohols, **3a–d**. Increased electron donations by 2,4,6-alkyl groups results in a downfield ^{17}O shift compared with that for benzyl alcohol, that increases with the bulk of the alkyl group. Interestingly the 1 ppm shift for the mesityl derivative **3b** is lower than expected from additivity of the polar effect since $\delta(^{17}O)$ values are 6.0 and 7.7 for $PhCH_2OH$ and *p*-$MeC_6H_4CH_2OH$ in toluene.[27] However, the shifts for the other alkyl groups are higher than predicted by electronic effect, and we conclude that both steric and electron-donation effects contribute to the downfield shifts.

Increased downfield shifts of $\delta(^{17}O)$ of aliphatic ROR′ with increased electron density on the oxygen was predicted by calculations and ascribed to a decreased ΔE.[29] This may also apply to $ArCH_2OH$ since the ΔE term dominates the $\delta(^{17}O)$ of aliphatic ROH.[30]

6a **6b**

α,β-Unsaturation in ethers causes a large downfield shift,[31] *e.g.*, $\delta(^{17}O)$ $CH_2{=}CHOMe$, 57.0;[31b] CH_3CH_2OMe, 22.5. This was ascribed to dipolar structure **6b**, which increases the $(r^{-3})_{2p_0}$ term in eqn. (1). Extended conjugation increases $\delta(^{17}O)$.[32]

Although increased electron donation of the alkyl group in alkyl vinyl ethers increases $\delta(^{17}O)$,[31b] the shifts in alcohols are higher than in methyl ethers,[13] as shown also for the pairs **1c**/**2a**, **1k**/**2c** and **1l**/**2b**. If we use values of 15.5 and 28 ppm upfield shifts for the Me *vs.* H difference, found for MeOH/MeOMe and n-ROH/n-ROMe respectively,[13] $\delta(^{17}O)$ in $H_2C{=}CHOH$ is in the range 72–85 ppm. This value is relevant to the value calculated below.

Until recently, only a few not intramolecularly bonded phenols were studied. Both *o*-electron donating (Me)[33] and withdrawing (NO_2)[30a] groups deshield the oxygen relative to *o*-H. Intramolecular hydrogen bonding result in downfield shifts, *e.g.* of 16 and 21 ppm in *o*-$C_6H_4(OH)CRO$, R=H, Me,[34] compared with PhOH. The recently published $\delta(^{17}O)$ values for 4-XC_6H_4OH in MeCN[9] change from 65.6 (*p*-H_2N) to 93.7 ppm (*p*-O_2N) and $\delta(^{17}O)$ [*o*-X] < $\delta(^{17}O)$ [*p*-X].

Electronic Effects on $\delta(^{17}O)$ *Values of Enols.*—The conclusion from the analogies above and other data is that increased charge density on a singly bonded oxygen by α-electron donating substituents is accompanied by a downfield shift of the $\delta(^{17}O)$ value when the oxygen is bound to an sp^3 carbon. Conjugation leads to a strong downfield shift compared with the saturated alcohols and when the oxygen is bound to an sp^2 carbon the electronic effect of *conjugated* substituents is opposite to that described above, *i.e.*, electron withdrawal causes a downfield shift.

Consequently, the effects of α- and β-substituents in our enols are different. Since R in **1** is attached to the central atom of a heteroallylic system and is not directly conjugated to the oxygen a downfield shift is expected on electron donation by α-substituents. The differences between $\delta(^{17}O)$ values for RCH_2OH for R = H, Bu^t, *p*-$CF_3C_6H_4$, Ph, *p*-$MeOC_6H_4$ [− 37, −6.5, 1.2 (neat), 6.0 and 10.3 (in toluene)] and 10 for R = Mes from the present work are mostly larger than those for the corresponding enols $Mes_2C{=}C(OH)R$ with the same R's (δ 73.5, 93.0, 87.4, 84.6, 86.6 and 98.5, respectively) and the order for sub-groups is nearly the same. Consequently, although the steric effect should also contribute (*cf.* the higher shift for R = Bu^t than for Ph in the enols), the electronic effect from C_α seems *at least* as important as the steric effect.

A Search for λ_{max} *Dependence of* $\delta(^{17}O)$.—A correlation with the lowest energy λ_{max} may be expected by eqn. (1).[7] From the UV data λ_{max} (**1f**) > λ_{max} (**1l**), λ_{max} (**1i**) > λ_{max} (**1c**). The complete order is unclear due to the uncertainty in the value of the longer λ_{max} (see above). However, since λ_{max} (**1f**) is the highest while the $\delta(^{17}O)$ shift of **1f** is of intermediate value, a correlation does not exist for the four enols. Since the highest λ_{max} probably involve transitions of the doubly bonded chromophore, the comparison above may be unjustified. However, no correlation was found with the λ_{max} of higher energy transitions.

$\delta(^{17}O)$ *Values and Aryl–C=C Torsional Angles.*—The appreciable $\delta(^{17}O)$ SCS for crowded aromatic nitro or carbonyl compounds compared with the non-crowded analog[8a,b] were ascribed to torsional angle changes between the conjugated probe group and the aromatic group. Linear $\delta(^{17}O)$ values *vs.* torsion angles correlations[8a,b] were explained by a change in electron density on oxygen with the change in conjugation.

Table 7 Ar–C=C Torsion angles and $\delta(^{17}O)$ values

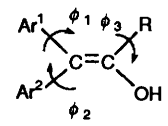

				Torsion Angle/°				
No.	Ar^1	Ar^2	R	φ_1	φ_2	φ_3	Ref.	$\delta(^{17}O)$
1a	Tip	Tip	H	58.9	54.4		15	70.5
1b	Br_2Mes	Br_2Mes	H	54.9	59.1	—	14	71.9
				58.9	60.3	—		
1c	Mes	Mes	H	50.2[a]	56.7[a]		3b, 35	73.5
1d	Me_5C_6	Me_5C_6	H	58.6	55.9	—	14	74.9
1f	Mes	Mes	Ph	62.43	65.7	33.3	36	84.6
1i	Mes	Mes	Bu^t	63.7	66.0	—	3b, 35	93.0
1j	Me_5C_6	Me_5C_6	Bu^t	61.7	61.4	—	14	94.1
1k	Ph	Mes	Mes	38.3	74.4	79.0	37	96.6
1l	Mes	Mes	Mes	52.5;	54.6;	52.7;	37	98.5
				51.4	58.2	55.6		

[a] Average value for the four symmetry independent crystallographic conformations.

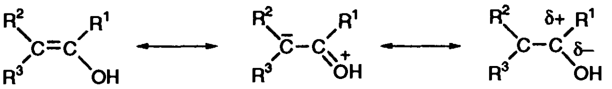

7a **7b** **7c**

The situation differs in our enols. The OH group is conjugated with the double bond and the resonance effect which is reflected by the contribution of hybrid **7b** makes the OH more positive and C-2 more negative than in analogous non-conjugated systems. Crystallography shows a nearly planar C=C–OH moiety and the C=C twist angle does not exceed 15° (in **1i**).[3b,35] The β-Ar–C=C conjugation should delocalize the negative charge on C-2 in **7b**, and hence changes in the β-Ar–C=C torsional angles (φ_1 and φ_2) should affect the observed shifts.

Crystallographic Ar–C=C torsion angles and $\delta(^{17}O)$ values for nine enols are given in Table 7. In the absence of other effects, the larger the torsion angles, the lower is the charge dispersal and the change in $\delta(^{17}O)$. For eight enols $|\varphi_1 - \varphi_2| < 7°$ and φ_1 and φ_2 for different enols do not differ much, being between 50.2 and 65.7. Hence, the extents of conjugation with the β-substituents are roughly similar. This also applies to **1k**, since in spite of a large $\varphi_1 - \varphi_2$ difference the $\varphi_1 + \varphi_2$ value resembles that in the other enols.

Since $\delta(^{17}O)$ changes by 28 ppm between **1a** and **l**, whose φ_1 and φ_2 values do not differ much, differences in conjugation and hence contribution of hybrid **7b** cannot be the main reason for the SCS in $CDCl_3$. Comparison of the $\delta(^{17}O)$ values of **1b**, **c** and **d** whose φ_1, φ_2 values are similar, corroborates this conclusion. The expectation, if conjugation is extensive, is for a less negative oxygen for **1b** and more negative oxygen for **1d** compared with **1c**. If $\delta(^{17}O)$ decreases for the less negative oxygen as found with α-substituents (but in contrast with phenols), the $\delta(^{17}O)$ values should be in the order **1d** > **1c** > **1b**. This is indeed observed. However, since the combined errors in the $\delta(^{17}O)$ values is of the order of magnitude of the observed change in the shifts, this precludes further conclusions from $\delta(^{17}O)$ values of **1b**–**d**.

That conjugation of the α-aryl group plays a small role, if at all, is shown by the close values of **1k** (φ_3 = 79°) and **1l** (φ_3 = 52.7° or 55.6°).

Solvent Effect.—From ^1H NMR and IR ν_{OH}, it was concluded that in low hydrogen bond accepting solvents such as $CDCl_3$ the OH group is hydrogen bonded to the π system of the *cis* aryl group in a *syn*-planar conformation.[4,5] This weak interaction probably causes a small constant downfield ^{17}O shift in the whole series compared with non-hydrogen bonded systems.[3] In a strong hydrogen bond accepting solvent such as DMSO this π(Ar)–HO interaction is replaced by a much stronger OH–DMSO hydrogen bonding in an anticlinal conformation.[4,5] This is reflected in the $\delta(^{17}O)$ values.

The $\Delta\delta O = \delta(^{17}O)([^2H_6]DMSO) - \delta(^{17}O)(CDCl_3)$ values decrease on increasing the bulk of R. For **1c** and **d** of group (*i*) where association with DMSO is the highest[4] $\Delta\delta O$ values are 7 and 10. For group (*ii*) enols **1e** and **f** where the association is weaker[5] the downfield shift is smaller, *ca.* 3 ppm. Unfortunately, the large error in $\delta(^{17}O)$ for **1i** in $[^2H_6]$DMSO and the absence of value for **1j** make $\Delta\delta O$ for α-*tert*-butyl enols unknown or highly unreliable. However, the average shift for **1i** is 1 ppm, *i.e.* smaller than for group (*ii*) enols. The largest $CDCl_3 \longrightarrow [^2H_6]DMSO$ change is a large *upfield shift* of 17 ppm for **1l**. Consequently, $\Delta\delta O$ values decrease continuously on increasing the bulk of R from group (*i*), *via* group (*ii*) to group (*iii*).

The solvent induced shift originates from a stronger hydrogen bonding to $[^2H_6]$DMSO, which causes shielding. The 11–14 ppm upfield $\delta(^{17}OH)$ shifts in $2\text{-}RC_6H_4OH$ compared with $4\text{-}RC_6H_4OH$, R = MeO, F were ascribed to intramolecular hydrogen bonding.[9,38]

Interestingly, the $\delta(^{17}O)$ shift of a simple hydroxy compound between two or more solvents is rarely studied.[39] The $\delta(^{17}O)$ values for two phenols in MeCN and toluene, differ very little.[40a] It was noted that 'the scarcity of comparable data does not allow us to identify the effect of H bonding upon the signal of an enol group.'[40b] Our values extended substantially the relevant data.

An interesting outcome of the different solvent-dependent $\Delta\delta O$ values for the three groups is that the subdivision in $CDCl_3$ no longer applies in $[^2H_6]$DMSO. Indeed, $\delta(^{17}O)([^2H_6]$-DMSO) for enol **1c** of group (*i*) and **1l** of group (*iii*) are almost identical, and for all the enols except **1j** $\delta(^{17}O) = 84.4 \pm 2.9$ ppm. Consequently, hydrogen bonding has an important effect on $\delta(^{17}O)$ values and may dominate over other effects. An explanation for the solvent dependence of the $\Delta\delta O$ values is given below.

^{13}C *Chemical Shifts.*—Many $\delta(^{13}C)$ values for hydrogen bonded enols are available.[6] Relevant comparisons of **1** are with other enols and with styrenes. Enols $p\text{-}XC_6H_4C^1OC^2H{=}C^3(Me)OH$[41] show δ(C-2) and δ(C-3) values at 95.6–98 and 191–196 ppm, respectively, with the higher values for electron-withdrawing X groups, as expected. Many other 1,3-diketones resonate in the same regions, but the $\delta(^{13}C)$ values may be averages for the C=O and C–OH signals due to intramolecular hydrogen bonding.

For simple enols $\delta(C_\beta) < \delta(C_\alpha)$. For $H_2C{=}CHOH$ $\delta(C_\beta) = 88$, $\delta(C_\alpha) = 149.0$ in 9:1 $CD_3CN\text{–}D_2O$,[42] for $CH_2{=}C(OH)\text{-}Me$[43] $\delta(C_\beta) = 95.3$, $\delta(C_\alpha) = 156.8$ in 2-PrOH and for $Cl_2C{=}CHOH$ $\delta(C_\beta){=}100$, $\delta(C_\alpha) = 141.3$ in 98:2 $(CD_3)_2CO\text{–}H_2O$.[44] Hence, neglecting solvent differences the β-Mes groups of **1c** decrease $\delta(C_\alpha)$ by *ca.* 5, but increase $\delta(C_\beta)$ by *ca.* 25 ppm. On increasing the bulk of R in **1** from H to Bu^t δ(C-1) increases by 11.8 ± 1.1 ppm and δ(C-2) decreases by 4.8 ± 0.4 ppm.

For styrenes the DSP correlations $C_\alpha(SCS) = -2.4\sigma_I - 0.4\sigma_R{}^\circ$; $C_\beta(SCS) = 5.0\sigma_I + 8.9\sigma_R$ indicate that C_α(SCS) are mainly influenced by the inductive effect and C_β(SCS) by the resonance effect.[19] However, it was suggested that the inductive effect also dominates $\delta(C_\beta)$.[18] Calculations show a relationship between SCS and π-electron densities at C_β. Donors on C_α induce a downfield shift, presumably by polarizing the vinyl π-cloud.[45]

Conjugation in the enols increases the electron density at C-2 (*cf.* **7b**) with a corresponding upfield shift of C-2. Indeed, large δ(C-1)–δ(C-2) differences are observed for ArC(CN)=CHOH, where C-2 carries the electron-withdrawing cyano group.[46]

An α-substituent effect on $\delta(^{13}C\text{-}2)$ was also observed for $RCH{=}CH_2$ where $\delta(^{13}C\text{-}2) = 110.2$ and 112.5 for R = Bu^t and Ph, respectively.[20b] The values for **1i** and **f** are rather similar, 108 and 111.5 ppm.

Qualitative models for the effect of the β-Mes groups on $\delta(^{13}C)$ are 9-methylene- or 9-arylmethylene-fluorenes Fl=CHR (Fl = 9-fluorenylidene), with *o*- and *m*-methyl groups.[47] An α-Ph shifts C_α downfield by 13–20 ppm and C_β upfield by 6–7 ppm. The steric hindrance of *o*-Me group causes only 3–4 ppm downfield shift compared with *m*-Me groups at C-2.

PM3 and IGLO Calculations.—Several important features arise from the PM3 calculations of charge densities and the IGLO calculations of $\delta(^{17}O)$ and $\delta(^{13}C)$ values. First, application of both the semiempirical method on our enols and the *ab initio* method for the simpler model give a parallel dependence of the charge density *q* on the torsional angle θ. Second, the *q* dependencies on θ for **1c**, **1f**, **1i** and **1l** are qualitatively similar. Third, the calculated ^{17}O shifts for **4** in the *syn* periplanar conformation **4a**, *i.e.*, 82.7 ppm is in the range estimated above from data on the methyl ethers. It is 10 ppm higher than the average for group (*i*) enols in $CDCl_3$, where the conformation is *syn*-periplanar.[4,5] From Table 4(*b*), (*c*) we conclude that this value will not be affected when the dielectric constant of $CDCl_3$ is used in the calculation. The discrepancy of the calculated $\delta(^{13}C\text{-}1)$ (175.8 ppm) and the observed (149.0 ppm) values for **4** or for **1a–d** (average 145.1 ppm) is much larger. For $\delta(^{13}C\text{-}2)$ (calc. 105.2 ppm; observed for **4**: 88.0 ppm, average for **1a–d** 113.7 ppm) it is somewhat lower. However, most of the discrepancy between the calculated and observed $\delta(^{13}C)$ values disappear when using the higher level GIAO[MPBT(2)]/*qzp*(C,O)*tzp*(H) calculations, which for **4a** give $\delta(^{13}C_\beta)$ 86.3, $\delta(^{13}C_\alpha)$ 155.5 ppm. $\delta(^1H)$ of **4a** is lower than the observed value [for **4** in 99% $(CD_3)_2CO$: 1% H_2O $\delta = 7.95$[42] probably due to intermolecular hydrogen bonding]. The value is close to that of enols **1** in $CDCl_3$ where π(Ar)–HO hydrogen bonding is weak.

Fourth, an α-methyl substituent, at all conformations studied increases $\delta(^{17}O)$ and $\delta(^{13}C\text{-}1)$ and decreases $\delta(^{13}C\text{-}2)$. This resembles the observed direction of change in R in **1** from H to Bu^t and is consistent with the corresponding shifts observed for alkenes.

Fifth, from Figs. 3 and 6, the more stable conformation of either the β,β-dimesityl-substituted enols or of ethenol **4** is the *syn* conformation, whereas the higher energy conformation is the perpendicular conformation. This reflects the importance of π(C=C)–p(O) conjugation which amounts to *ca.* 5 kcal mol^{-1}.

Sixth, the calculations [Figs. 10(*a*) and 11] show that both the charges and the ΔE term affect the $\delta(^{17}O)$ chemical shift but in opposite directions. Hence, a reciprocal relationship between the charge on an atom and its chemical shift does not apply for all the atoms. Table 4 shows that at all levels of calculation, with and without added solvent, such reciprocal relationship holds for C-2 and O at the three conformations **4a–c**. Apparently, for a single species, the conjugation, represented by hybrid **7b**, has the major effect on the charges and δs of the O and C-2 at the ends of the oxoallylic system. As in phenols, the more positively charged oxygen and more negatively charged C-2 in the *syn* conformation than in the perpendicular conformation results in a consequent upfield shift of the oxygen signal and a downfield shift of the carbon signal when conjugation is reduced by rotation of the OH group out of the C=C plane. At complete deconjugation when $\theta = 90°$ (**4b**), the charge density on O is the highest and on C-2 is the lowest, $\delta(^{17}O)$ is at a minimum and $\delta(^{13}C\text{-}2)$ is at a maximum.

In contrast, the relationships between the calculated charges at the non-conjugated C-1 and H and their chemical shifts are more complex. Both atoms are positively charged in the three conformations. The calculated charge densities at the hydrogen in the three conformations are nearly the same, but the $\delta(^1H)$ value for the perpendicular conformation is always lower than for the *syn* and *anti* conformations. Hence, the hydrogen shift parallels the oxygen shift although not linearly since the $\delta(^{17}O)$ *vs.* $\delta(^1H)$ plot has an exponential shape. The $\delta(^1H)$–θ dependence reflects the π(C=C)–p(O) conjugation whose effect on the oxygen charge is relayed to the hydrogen by polarization of the O–H bond.

For C-1, the perpendicular conformation is the less positively charged at all levels of calculation (or is identically charged in the *anti* conformer **4c**·O=SH$_2$ using SCRF). The shifts, however, decrease in the order δ(**4a**) > δ(**4b**) > δ(**4c**). This indicates that the charge on C-1 is influenced by the charges at the neighbouring C-2, R and oxygen (*cf.* structure **7c**). Apparently, this is a composite influence, resulting in a lack of a relationship between q(C-1) and $\delta(^{13}C\text{-}1)$.

Seventh, whereas the effect of the dielectric constant on the chemical shifts is small, hydrogen bonding to one H_2S=O molecule affects the various shifts, although to a different extent. The hydrogen bonding polarizes the O–H bond in the sense $O^{\delta-}\cdots H^{\delta+}$ calculationally, this leads to an appreciable downfield shift of $\delta(^1H)$ and upfield shift of $\delta(^{17}O)$ at all conformations.

A more negatively charged oxygen (in **4**·O=SH$_2$ *vs.* **4**) will delocalize the charge better to C-2 (*cf.* **7b**) and will reduce the contribution of **7c** with a consequent shift of $\delta(^{13}C\text{-}2)$ to an upper field and of $\delta(^{13}C\text{-}1)$ to a lower field. These changes are consistent with the observed ones (Table 4), except for a negligible change of −0.1 ppm for C-1 in **4a**·O=SH$_2$. Since the effect of conformation on $\delta(^{13}C\text{-}1)$ is small, the small ΔC-1 value (except for **4c**) is reasonable. However, the expectation is that ΔC-2 will be less influenced in the (p) conformation, where conjugation is minimal than in the (*a*) and (*s*) conformation, but this is not the case.

The effect of the hydrogen bonding is the largest for the hydrogen, the atom directly involved in the bonding and the downfield shift is appreciable, bringing $\delta(^1H)$ closer to the observed values for **1a–d**.

Finally, the difference in the q values for θ and $-\theta$ values are consistent with the chirality of the propeller Ar$_2$C=C and Ar$_2$C=C(Ar) moieties since molecules with θ and $-\theta$ are diastereoisomeric.

The Solvent Effect.—The substituent dependent observed solvent effect (ΔδO) on $\delta(^{17}O)$ cannot be explained by the calculation on a single simple molecule like **4**. However, the calculations indicate the complexity of the problem. We know from the ^3J(HCOH) values that hydrogen bonding changes the conformation from *syn*-periplanar present in CDCl$_3$ to *anti*-clinal in DMSO[4,5] and from the PM3 calculations that at *ca.* $\theta = 90°$ the oxygen is more negative and C-2 is less negative than when $\theta = 0$.

However, if the results of the *ab initio* calculations on **4** are applied in an attempt to explain the solvent effect on $\delta(^{17}O)$ of **1**, a problem arises. Complexation by solvent compared with uncomplexed *syn* **4a** without applying a reaction field predict a shift of the ^{17}O signal to a higher field (Table 4). However, such a shift is observed only for **1l**, but not for the other enols. We believe that an explanation has to neglect the extent of the shift while accepting the shape of the $\delta(^{17}O)$ *vs.* θ plot.

In view of the large downfield effect of conjugation on $\delta(^{17}O)$ values for ethers and phenols, and the extensive change in $\delta(^{17}O)$ with the change in θ, we believe that the trend shown in Fig. 8 is real, although the actual $\delta(^{17}O)$ values may differ from the calculated ones. Moreover, whereas an appreciable upfield shift is calculated for **4**·O=SH$_2$ compared with **4**, the shift becomes smaller using the SCRF method, and for the perpendicular and *anti* complexes, there is no effect if their combined experimental error in ΔδO (2 ppm) is taken into account. The shift is even slightly downfield for the α-substituted **5**·O=SH$_2$ (Table 5). In view of the discrepancy between the calculated (by IGLO) and observed shifts, the differences between DMSO and H$_2$SO, the effect of the basis set and the reaction field on the calculated shifts, the twist around the C=C bond in the more crowded enols, and the π(Ar)–HO bonding in them and especially the large structural difference between the simple model **4** and our enols we believe that at the present state we can neglect the calculation results that hydrogen bonding leads to a small shift in **4b**·O=SH$_2$ and **4c**·O=SH$_2$. Instead, we will use analogies and assume that hydrogen bonding in enols **1**, at a single conformation will cause downfield $\delta(^{17}O)$ shifts, as observed for phenols.

We then dissect the effect of association with [$^2H_6$]DMSO to three factors. (*a*) A conformational change which always decreases $\delta(^{17}O)$ from its maximal value of **4a** in CDCl$_3$, but more so for smaller $|90° - \theta|$ values. (*b*) Hydrogen bonding, which *we assume* to increase $\delta(^{17}O)$ values, and more so for the stronger association. (*c*) A steric effect at C-1 which decreases the $|90° - \theta|$ angle with the increase of the bulk of R.

For group (*i*) enols where the association is the strongest and the steric effect is the lowest, factor (*b*) dominates giving the highest ΔδO values. For group (*ii*) and for the *tert*-butyl enol **1i** the association constants K_{ass} for **1**·DMSO are lower than for **1c** for electronic and steric reasons {K_{ass} in [$^2H_6$]DMSO: 5.25 (**1c**);[4b] 1.93 (**1f**);[5] 0.47 (**1c**)[4b]}, and the order of K_{ass} values parallels the order of ΔδO values. The $|90° - \theta|$ value can also become smaller than for group (*i*), due to steric reasons. Enol **1i** exists as a rapidly equilibrating 13:87 mixture of *syn*-planar to *anti*-clinal conformations[4b] and the average θ of both conformations will also reduce the $|90° - \theta|$ value. Consequently, factors (*a*) and (*b*) nearly balance each other and ΔδO = 1–3.4 ppm.

K_{ass} for the α-mesityl enol **1l** (1.82 in DMSO[5]) resembles that for **1f** and association exceeds 98% in both cases. A reasonable explanation for the highly negative ΔδO value is that the $|90° - \theta|$ value is much smaller than for other enols due to a steric reason. In the **4b**-like perpendicular conformation, the geminal steric interaction of the bulky Mes and OH·DMSO moieties is maximally relieved. The negative ΔδO value is then due to a combination of factors (*a*)–(*c*), where (*a*) and (*c*) predominate over (*b*).

We note that except for group (*i*) enols, where approximate θ values may be evaluated from ^3J(HCOH) values we have no knowledge of the magnitude of θ. The presence of the anticlinal conformation in DMSO is deduced from data on **1a–d**, solid state crystallography of enol solvates and inspection of space-filling models. We also note that the difference in charges between the *syn* and the perpendicular conformations is the highest for **1c** and the lowest for **1l**. This factor should result in a different qualitative response of $\delta(^{17}O)$ to the conformation change on hydrogen bonding. However, since other effects on $\delta(^{17}O)$ are important, we cannot evaluate the importance of this effect.

Distinguishing steric and hydrogen-bonding effects could have been assisted by $\delta(^{17}O)$ data of ethers **2a–c** in CDCl$_3$ and [$^2H_6$]DMSO. Unfortunately, $\delta(^{17}O)$ values in [$^2H_6$]DMSO are unavailable. The values of 49–48 ppm for **2a** and anisole[31] and 56 for **2b** and **2c** in CDCl$_3$ are *ca.* 25 and 41 ppm lower than for the corresponding **1c**, PhOH, **1k** and **1l**. This is reminiscent of the differences of saturated alcohols from their methyl ethers[13] (26–29 ppm for primary, 41.8–51.8 ppm for secondary systems), so that values in a single solvent are insufficient to give mechanistic information.

If $\delta(^{17}O)$ and $\delta(^{13}C\text{-}2)$ values are strongly influenced by the mutual conjugation of the O and C-2, it is likely that the solvent induced shifts $\Delta\delta O$ and $\Delta\delta C\text{-}2$ (Table 1) should change in opposite directions. This is found for group (*i*) enols where the Δs are relatively large and for group (*ii*) enols and **1i** where both changes are small. However, trimesitylethenol **1l** is again an exception. Both the ^{17}O and the ^{13}C-2 signals shift to high field in DMSO. Consequently, the lack of complete parallel in ^{17}O and ^{13}C-2 SCS extends to the solvent change.

$\delta(^{1}H)$–$\delta(^{17}O)$, $\delta(^{13}C)$–$\delta(^{13}C)$ *and* $\delta(^{13}C)$–$\delta(^{17}O)$ *Correlations.*—$\delta(^{1}H)$ and $\delta(^{17}O)$ of the OH group of phenols are linearly correlated.[16] For many alcohols ROH, $\delta(^{17}O)$ is linearly correlated with $\delta(^{13}C)$ [RCH_3].[33] Consequently, we searched for similar correlations of our data.

In $CDCl_3$ the $\delta(^{17}O)$ and $\delta(^{1}H)$ values for groups (*i*) and (*ii*) cluster in two relatively narrow regions with no linearity for the four points of each group. The δ values for group (*ii*) are higher than for group (*i*). The values for group (*iii*) show large dispersion. The negative slope of the $\delta(^{17}O)$ *vs.* $\delta(^{1}HO)$ linear correlation for five enols in [$^{2}H_6$]DMSO indicates, as expected, opposite charges on the OH hydrogen and the oxygen of the hydrogen bonded species.

The lack of good linearity for all points indicates that part of the effects operating on both nuclei are different. For example, the ring current effect of the aryl groups on $\delta(^{1}H)$ is presumably more appreciable than on oxygen.[48]

$\delta(^{13}C)$ *vs.* $\delta(^{17}O)$ correlations are not necessarily expected, since the shifts are influenced by a different combination of effects for both nuclei.[49] However, if **7b** is important the SCS at ^{17}O and C-2 should be parallel in opposite directions; such a relationship is not expected at C-1.

Only a rough correlation having a negative slope does exist between $\delta(^{17}O)$ and $\delta(^{13}C\text{-}2)$ for group (*i*) enols but the other points show complete scatter [Fig. 1(*b*)]. The rough $\delta(^{17}O)$ *vs.* $\delta(^{13}C\text{-}1)$ correlation of Fig. 1(*a*) mainly reflects clustering of substituents of each of groups (*i*) and (*ii*). The positive slope is accounted for if both hybrids **7b** and **c** are important, since then the $\delta(^{17}O)$ and $\delta(^{13}C\text{-}1)$ SCS may be in the same direction.

The linear correlation between $\delta(^{13}C\text{-}1)$ values in $CDCl_3$ and [$^{2}H_6$]DMSO is not surprising. C-1 is the atom least influenced by conjugation, and the correlation probably indicates a general medium effect. The observation of two parallel lines with deviation of **1l** in the $\delta(^{13}C\text{-}2)$ [$CDCl_3$] *vs.* $\delta(^{13}C\text{-}2)$ ([$^{2}H_6$]-DMSO) correlation indicates a specific effect on C-2. A different degree of conjugation for the more strongly associated α-H enols then for the more hindered α-alkyl and α-aryl enols may contribute to the dispersion to two lines.

The $\delta(^{13}C)$ values for styrenes and group (*ii*) enols are very similar so that the effects of the α-OH and the two β-mesityl groups cancel each other. Correlation of $\delta(^{13}C\text{-}1)$ for **1** with $\delta(C_\alpha)$ of the styrenes[17,18] is nonlinear while a $\delta(C_\beta)$ [styrenes] *vs.* $\delta(C_2)$ (**1**) plot is linear. The Hammett correlation for $\delta(^{13}C\text{-}2)$ of group (*ii*) resembles DSP correlations for styrenes and is due to the operation of electronic effects.

Conclusions.—The $\delta(^{17}O)$ values for enols **1a**–**1l** in $CDCl_3$ are divided into three groups which parallel the increased bulk of the α-substituents. The values are influenced by several effects. Polar effects strongly influence the changes R = H ⟶ R = Bu^t, or those for *m*- and *p*-substituted α-Ar groups. Resonance effects, manifested by hybrid **7b** are important and conformation-dependent, but like the π(Ar)–OH hydrogen bonding are not demonstrated *in* $CDCl_3$ where the conformation and Ar–C=C torsional angles θ are approximately similar for all the enols. The calculated $\delta(^{17}O)$ values are sensitive to the conformation of the C=C–O–H moiety, due to the dependence of the π(C=C)–n(O) conjugation on θ. The change of the solvent to [$^{2}H_6$]DMSO results in $\Delta\delta O$ values that are positive for group (*i*) enols but decrease with the increase bulk of R, up to −17.4 for **1l**. This results from a compromise between hydrogen bonding to [$^{2}H_6$]DMSO which increase $\delta(^{17}O)$, accompanied by a conformational change to a more perpendicular C=C–O–H conformation and a lower $\delta(^{17}O)$, which depends on the bulk of the α-substituent.

Experimental

Materials.—Most of the enols and ether **2c** were available from previous studies or prepared by known methods.[3a,4,14,15,36] 2,4,6-trimethyl[50a] and 2,4,6-triisopropyl[51b] benzyl alcohols **3b** and **3c** were prepared by $LiAlH_4$ reduction of the corresponding aldehydes and 2,4,6-tri-*tert*-butylbenzyl alcohol was prepared by reduction of the corresponding formate.[51] UV spectra were measured on a UVIKON 930 (Kontron Instruments) and Hitachi U-3410 spectrometer.

2,2-*Dimesitylvinyl methyl ether* (**2a**).—To a solution containing 2,2-dimesitylethenol **1c** (234 mg, 0.84 mmol) and Bu_4NBr (50.5 mg, 0.16 mmol) in methyl iodide (4.8 cm^3) was added to a solution of 50% aqueous NaOH (9 cm^3) and the mixture was stirred overnight at room temperature. Diethyl ether (45 cm^3) was then added, the phases were separated and the organic phase was washed with water (3 × 30 cm^3), dried ($MgSO_4$), and evaporated, giving a colourless solid, mp 126–128 °C (196 mg, 80%). Crystallization from light petroleum (40–60 °C) gave colourless crystals (155 mg, 63%) of dimesitylvinyl methyl ether, mp 128–128.5 °C; $\delta_H(CDCl_3$, rt) 2.09, 2.24 (2s) and broad coalescing signals at 1.77 and 2.56 (total 18H, Me), 3.70 (3 H, s, OMe), 6.11 (1 H, s, =CH) and 6.81 (4 H, s + br coalescence signal, Ar-H); $\delta_H(CDCl_3$, 213 K) 1.78, 1.80 (6 H, 1s, 1 br s, 2 Me), 2.26, 2.28 (6 H, 2s, 2 Me), 2.41 (*ca.* 3 H, br s, Me), 2.60 (3 H, s, Me), 3.74 (3 H, s, OMe), 6.14 (1 H, s, =CH), 6.76 (2 H, 1 br s, 2 Ar-H), 6.98 and 7.02 (2 H, 1 br s, 1s, 2 Ar-H); *m*/*z* (%, assignment): 294 (100, M), 279 (8, M − Me), 264 (6, M − 2 Me), 263 (5, M − MeO), 251 (8, Mes_2CH), 249 (29, M − 3 Me), 247 (45, M − 2 Me − MeO), 234 (26, M − 4 Me), 221 (7), 159 (7), 131 (11), 116 (9) and 91 (6) (Found: C, 85.8; H, 8.7. Anal. Calc. for $C_{21}H_{26}O$: C, 85.66; H, 8.90%.)

Methyl Trimesitylvinyl Ether (**2b**).—To a solution containing trimesitylethenol **1l** (150 mg, 0.375 mmol) and Bu_4NBr (32 mg, 0.1 mmol) in methyl iodide (2.9 cm^3) was added a solution of 50% aqueous NaOH (7 cm^3) and the mixture was stirred for 20 h at room temp. Diethyl ether (35 cm^3) was added, the phases were separated and the organic phase was washed with water (3 × 20 cm^3), dried ($MgSO_4$) and evaporated, giving a colourless solid (109 mg, 81%), mp 110–111 °C. δ_H 1.82, 1.85, 1.86, 1.92, 2.13, 2.23, 2.24, 2.37, 2.57 (27 H, 9s, Me), 3.24 (3 H, s, OMe), 6.54, 6.60, 6.63, 6.72, 6.87 and 6.97 (6 H, 6s, Ar–H). Crystallization from *n*-pentane gave white crystals of methyl trimesitylvinyl ether (106 mg, 80%), mp 162–163 °C (lit.,[52] 162–163 °C).

NMR Spectral Measurements.—^{17}O NMR spectra were measured on a Bruker AM360 spectrometer at 48.8 MHz in 10 mm φ sample tube containing 100 mg cm^{-3} in $CDCl_3$ or 100–200 mg cm^{-3} in [$^{2}H_6$]DMSO of each enol. The signals were referenced to external $H_2{}^{17}O$. All spectra were acquired at 50 °C in $CDCl_3$ and at 80 °C in [$^{2}H_6$]DMSO. The enols had natural abundance ^{17}O. The following acquisition parameters were typically used: 20 μs pulse width, 100 μs acquisition delay time, 18.4 ms acquisition time, 1 K data points, 28 kHz spectral width; and 100 000–3 000 000 transients. The spectral resolution was enhanced by the application of a Gaussian weighting function. The data resolution was improved to ±0.6 ppm by zero filling to 2K–4K data points. The reproducibility of the chemical shift data is estimated to be < ±1.0 ppm.

^{13}C NMR spectra were measured on a Bruker AM360 spectrometer at 90.56 MHz for 5 mm φ sample tube containing each enol in $CDCl_3$ or $[^2H_6]$DMSO. The solution which had been prepared for ^{17}O NMR measurements in $CDCl_3$ was utilized and the spectra were acquired at room temperature. In $[^2H_6]$DMSO, a solution of *ca.* 10 mg in 5 cm^3 solvent was prepared for each enol and ^{13}C NMR measurements were conducted at 30 °C. The signals were referenced to internal TMS. All spectra were acquired at room temp. The following acquisition parameters were used: 3 μs pulse width, 32K data points, 20 kHz spectral width and 1000–4000 transients. The digital resolution was ±0.014 ppm.

Ab initio *and Semiempirical PM*3 *Calculations*.—(*a*) Ab initio *calculations*. Standard *ab initio* molecular orbital calculations[53] were carried out with a version of the GAUSSIAN 92 program.[54] Geometry optimizations were performed with the 6-311G** basis set[55a] with electron correlation incorporated using second order Moller–Plesset perturbation theory[55b] (MP2/6-311G**). For the geometry optimizations of the larger complexes we used the smaller 6-31G** basis.[55c]

The IGLO calculations of NMR chemical shifts[56a] were performed using the basis II[56b] for oxygen and carbon and DZ[56b] for hydrogen. This combination of basis sets is referred to as basis II′ throughout the text. The GIAO/MBPT(2) calculations[58] were done with the ACES II program system[57] using the *qzp* basis set[59] for oxygen and carbon and the *tzp* basis[59] for hydrogen.

The NBO analysis was conducted using the NBO Version 3.1[60] as implemented in the GAUSSIAN 92 program.

In order to model the influence of the solvent on the calculated geometries, we used the Self Consistent Reaction Field method (SCRF).[61] We conducted geometry optimizations at the Hartree–Fock level using the 6-311G** basis set in the presence of a reaction field with dielectric constants $\varepsilon = 4.17$ and $\varepsilon = 46.7$ as models for the solvents $CDCl_3$ and DMSO, respectively. The geometries of the complexes were only reoptimized for a medium with a dielectric constant $\varepsilon = 46.7$ at the HF/6-31G** level. For the optimized geometries the chemical shifts were calculated using the IGLO method.

(*b*) *PM*3 *Calculations*. All calculations were carried out (using program ANCHOR2 on a Fujitsu S-4/2 computer) by using the recently described PM3 semiempirical molecular orbital procedure[62] as implemented in the MOPAC 6 program package. The geometries of all species were fully optimized using the EF method[63] with no geometrical constraints except for a CCOH torsional angle.

Acknowledgements

We are indebted to Professors P. v. R. Schleyer and Y. Apeloig for discussions. J. F. thanks the A. Gal Memorial Fund and T. M. thanks the Minerva Foundation for fellowships.

References

1 Stable simple enols. Part 35. For part 34 see I. Eventova, E. B. Nadler, J. Frey and Z. Rappoport, *J. Phys. Org. Chem.*, 1994, **7**, 28.

2 (*a*) For reviews see H. Hart, Z. Rappoport and S. E. Biali, in *The Chemistry of Enols*, ed. Z. Rappoport, Wiley, Chichester, 1990, ch. 8, pp. 483–589. (*b*) Z. Rappoport and S. E. Biali, *Acc. Chem. Res.*, 1988, **21**, 442.

3 (*a*) D. A. Nugiel and Z. Rappoport, *J. Am. Chem. Soc.*, 1985, **107**, 3669; (*b*) S. E. Biali, D. A. Nugiel and Z. Rappoport, *J. Am. Chem. Soc.*, 1989, **111**, 846.

4 (*a*) S. E. Biali and Z. Rappoport, *J. Am. Chem. Soc.*, 1984, **106**, 5641; (*b*) Z. Rappoport, D. A. Nugiel and S. E. Biali, *J. Org. Chem.*, 1988, **53**, 4814.

5 E. B. Nadler and Z. Rappoport, *J. Am. Chem. Soc.*, 1989, **111**, 213.

6 See B. Floris, in *The Chemistry of Enols*, ed. Z. Rappoport, Wiley, Chichester, 1990, ch. 4, pp. 148–305.

7 *^{17}O NMR Spectroscopy in Organic Chemistry*, ed. D. W. Boykin, CRC Press, Boca Raton, Fl., 1991.

8 (*a*) D. W. Boykin and A. L. Baumstark, in ref. 7, ch. 3, p. 39; (*b*) *Tetrahedron*, 1989, **45**, 3613; (*c*) A. L. Baumstark and D. W. Boykin, in ref. 7, ch. 4.

9 D. W. Boykin, S. Chandrasekaran and A. L. Baumstark, *Magn. Reson. Chem.*, 1993, **31**, 489.

10 (*a*) H. A. Christ, P. Diehl, H. R. Schneider and H. Dahn, *Helv. Chim. Acta*, 1961, **44**, 865; (*b*) H. A. Christ and P. Diehl, *Helv. Phys. Acta*, 1963, **36**, 170.

11 M. Gorodetsky, Z. Luz and Y. Mazur, *J. Am. Chem. Soc.*, 1967, **89**, 1183.

12 V. V. Lapachev, I. Y. Mainagashev, S. A. Stekhova, M. A. Fedotov, V. P. Krivopalov and V. P. Mamaev, *J. Chem. Soc., Chem. Commun.*, 1985, 494.

13 S. Chandrasekaran, in ref. 7, ch. 7, pp. 141–203.

14 I. Eventova, E. B. Nadler, E. Rochlin, J. Frey and Z. Rappoport, *J. Am. Chem. Soc.*, 1993, **115**, 1290.

15 J. Frey and Z. Rappoport, unpublished results.

16 G. Jaccard and J. Lauterwein, *Helv. Chim. Acta*, 1986, **69**, 1469.

17 D. A. R. Happer and B. E. Steenson, *J. Chem. Soc., Perkin Trans. 2*, 1988, 19.

18 D. A. R. Happer, *J. Chem. Soc., Perkin Trans. 2*, 1984, 1673.

19 C. E. Aun, T. J. Clarkson and D. A. R. Happer, *J. Chem. Soc., Perkin Trans. 2*, 1990, 645.

20 H.-O. Kalinowski, S. Berger and S. Braun, *Carbon*-13 *NMR Spectroscopy*, Wiley, Chichester, 1988 (*a*) pp. 132–133; (*b*) p. 295.

21 M. Karplus and J. A. Pople, *J. Chem. Phys.*, 1963, **38**, 2803.

22 M. G. Oakley and D. W. Boykin, *J. Chem. Soc., Chem. Commun.*, 1986, 439.

23 A. L. Baumstark, P. Balakrishnan, M. Dotrong, C. J. McCloskey, M. G. Oakley and D. W. Boykin, *J. Am. Chem. Soc.*, 1987, **109**, 1059.

24 M. A. Wysocki, P. W. Jardon, G. J. Mains, E. J. Eisenbraun and D. W. Boykin, *Magn. Reson. Chem.*, 1987, **25**, 331.

25 D. W. Boykin, P. Balakrishnan and A. L. Baumstark, *Magn. Reson. Chem.*, 1985, **23**, 695.

26 M. Manoharan and E. L. Eliel, *Magn. Reson. Chem.*, 1985, **23**, 225.

27 P. Balakrishnan, A. L. Baumstark and D. W. Boykin, *Tetrahedron Lett.*, 1984, **25**, 169.

28 (*a*) A. C. Rojas and J. K. Crandall, *J. Org. Chem.*, 1975, **40**, 2225; (*b*) G. E. Maciel, *J. Phys. Chem.*, 1965, **69**, 1947; J. C. Bromilow, R. T. C. Brownlee, D. J. Craik, P. R. Fiske, J. E. Rowe and M. Sadek, *J. Chem. Soc., Perkin Trans. 2*, 1981, 753.

29 M.-T. Beraldin, E. Vauthier and S. Fliszar, *Can. J. Chem.*, 1982, **60**, 106.

30 (*a*) T. Sugawara, Y. Kawada, M. Katoh and H. Iwamura, *Bull. Chem. Soc. Japan*, 1979, **52**, 3391; (*b*) C. Delseth and J.-P. Kintzinger, *Helv. Chim. Acta*, 1978, **61**, 1327.

31 (*a*) M. Katoh, T. Sugawara, Y. Kawada and H. Iwamura, *Bull. Chem. Soc. Japan*, 1979, **52**, 3475; (*b*) E. Taskinen and J. Hellman, *Magn. Reson. Chem.*, 1994, **32**, 353.

32 (*a*) J. P. Kintzinger, C. Delseth and T. T.-T. Nguyen, *Tetrahedron*, 1980, **36**, 3431; (*b*) G. A. Kalabin and D. F. Kushnarev, *Dokl. Akad. Nauk SSSR*, 1980, **254**, 1425.

33 (*a*) J. K. Crandall and M. A. Cateno, *J. Org. Chem.*, 1979, **44**, 1183; (*b*) M. Takasuka, *J. Chem. Soc., Perkin Trans. 2*, 1981, 1558.

34 T. E. St. Amour, M. I. Burger, B. Valentine and D. Fiat, *J. Am. Chem. Soc.*, 1981, **103**, 1128.

35 M. Kaftory, D. A. Nugiel, S. E. Biali and Z. Rappoport, *J. Am. Chem. Soc.*, 1989, **111**, 8181.

36 E. B. Nadler and Z. Rappoport, *J. Am. Chem. Soc.*, 1987, **109**, 2112.

37 M. Kaftory, S. E. Biali and Z. Rappoport, *J. Am. Chem. Soc.*, 1985, **107**, 1701.

38 When the $\delta(^{17}O)$ of the hydroxy group of *o*-hydroxy- and *p*-hydroxybenzaldehydes are compared the former shows a signal at a

higher field (ref. 34), but the torsion angles effect should be taken into account.

39 A. L. Baumstark and D. W. Boykin, in ref. 7, ch. 5, pp. 95–114.

40 (*a*) D. W. Boykin, A. L. Baumstark and M. Beeson, *J. Org. Chem.*, 1991, **56**, 1969; (*b*) J.-C. Zhuo, H. Wyler, P. Pechy and H. Dahn, *Helv. Chim. Acta*, 1994, **77**, 317.

41 R. M. Cravero, M. Gonzales-Sierra and A. C. Olivieri, *J. Chem. Soc., Perkin Trans. 2*, 1993, 1.

42 B. Capon, D. S. Rycroft, T. W. Watson and C. Zucco, *J. Am. Chem. Soc.*, 1981, **103**, 1761.

43 (*a*) S. A. Sojka, C. F. Poranski, Jr. and W. B. Moniz, *J. Magn. Reson.*, 1976, **23**, 417; (*b*) W. B. Moniz, S. A. Sojka, C. F. Poranski and D. E. Birkle, *J. Am. Chem. Soc.*, 1975, **97**, 5953; 1978, **100**, 7940.

44 B. Capon, A. K. Siddhanta and C. Zucco, *J. Org. Chem.*, 1985, **50**, 3580.

45 D. A. R. Happer, *J. Chem. Soc., Perkin Trans. 2*, 1984, 1673.

46 G. Kirsch, J. L. Mieloszynski, D. Paquer and C. G. Andrieu, *Recl. Trav. Chim. Pays Bas.*, 1983, **102**, 489.

47 R. Knorr, D. S. Stephenson, P. Bohrer and T. P. Hoang, *Magn. Reson. Chem.*, 1993, **31**, 388.

48 G. A. Kalabin, D. F. Kushnarev, R. B. Valeyev, B. A. Trofimov and M. A. Fedotov, *Org. Mag. Reson.*, 1982, **18**, 1.

49 H. Dahn, P. Pechy and H. J. Bestmann, *J. Chem. Soc., Perkin Trans. 2*, 1993, 1497.

50 (*a*) R. C. Fuson, P. L. Southwick and S. P. Rowland, *J. Am. Chem. Soc.*, 1944, **66**, 1109; (*b*) R. C. Fuson, E. C. Horning, M. L. Ward, S. P. Rowland and J. L. March, *J. Am. Chem. Soc.*, 1942, **64**, 30.

51 A. Rieker, Y. Butsugan and M. Shimizu, *Tetrahedron Lett.*, 1971, 1905.

52 P. S. Bailey, J. W. Ward, R. E. Hornish and F. E. Potts, III, *Adv. Chem. Ser.*, 1972, **112**, 1.

53 W. J. Hehre, L. Radom, P.v.R. Schleyer and J. A. Pople, *Ab Initio Molecular Orbital Theory*, Wiley, New York, 1986.

54 M. J. Frish, G. W. Trucks, M. Head-Gordon, P. M. Gill, M. W. Wong, J. B. Foresman, B. G. Johnson, H. B. Schlegel, M. A. Robb, E. S. Repogle, R. Gomperts, J. L. Andres, K. Raghavachari, J. S. Binkley, C. Gonzalez, R. L. Martin, D. J. Fox, D. J. Defrees, J. Baker, J. J. P. Stewart and J. A. Pople, *Gaussian 92, Revision A*, Gaussian, Inc. Pittsburgh, PA, 1992.

55 (*a*) R. Krishnan, M. J. Frisch and J. A. Pople, *J. Chem. Phys.*, 1980, **72**, 4244; (*b*) C. Moller and M. S. Plesset, *Phys. Revs.*, 1934, **46**, 618; (*c*) P. C. Hariharan and J. A. Pople, *Chem. Phys. Lett.*, 1972, **66**, 217.

56 W. Kutzelnigg, U. Fleischer and M. Schindler, *NMR Basic Princ. Prog.*, 1990, **23**; (*a*) pp. 165–262; (*b*) pp. 190–191.

57 ACES II: J. F. Stanton, J. Gauss, J. D. Watts, W. J. Lauderdale and R. J. Bartlett, Quantum Theory Project, Departments of Chemistry and Physics, University of Florida, Gainesville, Florida.

58 GIAO method: R. Ditchfield, *Mol. Phys.*, 1974, **27**, 789; K. Wolinski, J. F. Hinton and P. Pulay, *J. Am. Chem. Soc.*, 1990, **112**, 8251. MBPT(2)/GIAO: J. Gauss, *Chem. Phys. Lett.*, 1992, **191**, 614; *J. Chem. Phys.*, 1993, **99**, 3629.

59 A. Schaefer, H. Horn and R. Ahlrichs, *J. Chem. Phys.*, 1991, **97**, 2751.

60 A. F. Reed, I. A. Curtiss and F. Weinhold, *Chem. Rev.*, 1988, **88**, 899.

61 M. W. Wong, M. J. Frisch and K. B. Wiberg, *J. Am. Chem. Soc.*, 1991, **113**, 4776; M. W. Wong, K. B. Wiberg and M. J. Frisch (*a*) *J. Chem. Phys.*, 1991, **95**, 8991; (*b*) *J. Am. Chem. Soc.*, 1992, **114**, 523; 1645.

62 J. J. P. Stewart, *J. Comput. Chem.*, 1989, **10**, 209.

63 J. Baker, *J. Comput. Chem.*, 1986, **7**, 385.

Paper 4/04402I
Received 18*th July* 1994
Accepted 4*th October* 1994